The Canadian Mineralogist
Vol. 46, pp. 87-109 (2008)
DOI: 10.3749/canmin.46.1.87

GEOCHEMISTRY AND ORIGIN OF CALCIC TUNGSTEN-BEARING SKARNS, LOS SANTOS, CENTRAL IBERIAN ZONE, SPAIN

FERNANDO TORNOS[§]

Instituto Geológico y Minero de España, c/Azafranal 48, E–37001 Salamanca, Spain

CARMEN GALINDO

Departmento de Petrología y Geoquímica, Universidad Complutense de Madrid, E–28040 Madrid, Spain

JOSÉ LUIS CRESPO

SIEMCALSA, c/Incas, 5, E–47008 Valladolid, Spain

BARUCH F. SPIRO

Department of Mineralogy, The Natural History Museum, Cromwell Road, London SW7 5BD, United Kingdom

ABSTRACT

The mesozonal, calcic and reduced Los Santos skarn, in the Central Iberian Zone, is a low-tonnage, high-grade tungsten deposit that occurs as discontinuous stratabound lenses enriched in scheelite along the contact between Variscan granodiorite–monzogranite and early Cambrian calcic and dolomitic marble and calc-silicate and pelitic hornfelses. The $\delta^{18}O$ values of the garnet and clinopyroxene in the prograde skarn are indicative of $\delta^{18}O_{fluid}$ compositions near 9.5–10.9‰. The compositions of clinoamphibole and biotite of the retrograde skarn suggest equivalent $\delta^{18}O_{fluid}$ values (9.1–12.0‰). These heavy $\delta^{18}O$ values indicate that the mineralizing fluids equilibrated with deep crustal rocks, with no significant input of surficial waters, even during the formation of the retrograde skarn. The Sr and Nd radiogenic isotope data for the scheelite ($^{87}Sr/^{86}Sr$ in the range 0.7117–0.7119; εNd_{300Ma} between –9.4 and –8.5), garnet–pyroxene skarn ($^{87}Sr/^{86}Sr$ in the range 0.7119–0.7128; εNd_{300Ma} between –8.5 and –8.7) and plagioclase-rich skarn ($^{87}Sr/^{86}Sr$ in the range 0.7124–0.7129; εNd_{300Ma} between –9.7 and –7.0) trace the complex evolution of hydrothermal fluids circulating through deep perigranitic systems. These signatures, as well as the REE contents, suggest equilibration of an external fluid with the host metasedimentary sequence. The regional geology and the Nd isotopes indicate that the ultimate source of the hydrothermal fluids and the tungsten and fluorine is not the adjacent barren granodiorite–tonalite nor the host metamorphic rocks, but rather an unexposed granitic pluton geochemically equivalent to the (biotite ± tourmaline)-bearing, fine-grained leucogranite dikes that crop out nearby. These are characterized by high ^{87}Sr values ($^{87}Sr/^{86}Sr > 0.7112$–0.7149) and intermediate εNd signatures (εNd_{300Ma} in the range –5.6 to –4.6) and are similar to those hosting perigranitic W–(Sn) mineralization in other areas of the Variscan Belt. Thus, the geochemical data show that the magmatic fluids extensively interacted with the host aluminosilicate rocks but were not able to precipitate the scheelite and fluorite until the reaction with carbonate rocks. Scheelite from nearby regionally stratabound orebodies have isotopic signatures ($^{87}Sr/^{86}Sr$ in the range 0.7108–0.7110; εNd_{300Ma} = –8.6) similar to those of the Los Santos skarn, strongly suggesting that they are also of Variscan perigranitic origin and not exhalative or synmetamorphic, as had been previously proposed.

Keywords: scheelite, isotope geochemistry, skarn, leucogranite, Spanish Central System, Los Santos deposit, Spain.

SOMMAIRE

La skarn de Los Santos, mésozonale, calcique et réductrice, affleurant dans la Zone Ibérique Centrale, constitue un gisement de tungstène à tonnage limité mais à teneur élevée se présentant en lentilles enrichies en scheelite le long du contact entre granodiorite–monzogranite varisque et marbres calcique et dolomitique, calc-silicates et cornéennes pélitiques d'âge cambrien précoce. Les valeurs de $\delta^{18}O$ du grenat et du clinopyroxène dans la skarn prograde indiqueraient des valeurs $\delta^{18}O$ de la phase fluide voisines de 9.5–10.9‰. La composition de la clinoamphibole et de la biotite des skarns rétrogrades indiqueraient des valeurs de $\delta^{18}O$ de la phase fluide équivalentes (9.1–12.0‰). Ces valeurs élevées de $\delta^{18}O$ montrent que les fluides minéralisateurs

§ *E-mail address*: f.tornos@igme.es

ont équilibré avec des roches crustales profondes, sans signes d'une interaction avec des eaux de surface, même pas au cours de la formation des skarns rétrogrades. Les données isotopiques pour le Sr et le Nd dans la scheelite ($^{87}Sr/^{86}Sr$ entre 0.7117 et 0.7119; εNd_{300Ma} entre –9.4 et –8.5), le skarn à grenat–pyroxène ($^{87}Sr/^{86}Sr$ entre 0.7119–0.7128; εNd_{300Ma} entre –8.5 et –8.7) et les skarns riches en plagioclase ($^{87}Sr/^{86}Sr$ entre 0.7124 et 0.7129; εNd_{300Ma} entre –9.7 et –7.0) tracent l'évolution complexe de fluides hydrothermaux lors de leur circulation au travers de socles périgranitiques profonds. D'après ces signatures, de même que les teneurs en terres rares, il y a eu équilibrage d'un fluide externe avec les roches hôtes métasédimentaires. Le contexte géologique régional et les données sur les isotopes de Nd indiquent que la source des fluides hydrothermaux, du tungstène et du fluor n'est pas la granodiorite–tonalite adjacente mais stérile, ni les roches hôtes métamorphiques, mais plutôt un pluton granitique évolué enfoui, géochimiquement équivalent des filons leucoranitiques à biotite ± tourmaline, à granulométrie fine, qui affleurent tout près. Ces filons possèdent une teneur élevée en ^{87}Sr ($^{87}Sr/^{86}Sr > 0.7112–0.7149$) et une valeur intermédiaire de εNd (εNd_{300Ma} entre –5.6 et –4.6), et ressemblent aux roches périgranitiques hôtes de minéralisation W–(Sn) ailleurs dans la ceinture varisque. Les données géochimiques montrent donc que ces fluides ont longuement interagi avec les roches hôtes aluminosilicatées, sans pouvoir précipiter la scheelite et la fluorite avant de réagir avec des roches carbonatées. La scheelite provenant des gisements régionalement développés en strates dans le voisinage ont des signatures isotopiques ($^{87}Sr/^{86}Sr = 0.7108–0.7110$; $\varepsilon Nd_{300Ma} = –8.6$) semblables à celles de la skarn de Los Santos, ce qui nous pousse à l'attribuer aussi aux venues périgranitiques varisques, et non aux phénomènes exhalatifs ou synmétamorphiques, comme on l'avait proposé antérieurement.

(Traduit par la Rédaction)

Mots-clés: scheelite, géochimie isotopique, Zone Ibérique Centrale, skarn, leucogranite, gisement de Los Santos, Espagne.

Introduction

Skarns are one of the major sources of tungsten, a feature that has encouraged systematic exploration and extensive study worldwide (*e.g.*, Einaudi *et al.* 1981, Kwak 1987, Meinert 1993). Tungsten-rich skarn deposits are usually located at the contact between intermediate to acid plutonic rocks and limestone or other Ca-rich lithologies. Knowledge of the source of metals and fluids is of prime interest for understanding how and where the ore deposits are formed; despite a plethora of studies on the origin of base metals and gold, there is little research on W and Sn.

The Iberian Peninsula has been one of the leading tungsten-producing zones of Europe. Most of the tungsten mineralization is located in a) granite-related ferberite- and scheelite-rich veins and greisens, b) stratabound scheelite mineralization within metamorphic belts, and c) tungsten-bearing skarns (*e.g.*, IGME 1985, Tornos & Gumiel 1992, and references therein). By far most of the historical production comes from the veins and greisens. Scheelite-bearing skarns have been described in the internal zones of the Variscan Belt and in the Pyrenees (Guy 1979, Soler 1980, Casquet & Tornos 1984, 1991, Soler *et al.* 1990, Gaspar & Inverno 2000), but only a few of them have been of economic significance. However, this situation changed dramatically when the Los Santos deposit was discovered and evaluated in 1980–1986 in a Billiton Española S.A. – Promotora de Recursos Naturales SA joint venture oriented to the regional exploration for tungsten-bearing skarns in areas with no previous record of such mineralization. Nowadays, current total resources of Los Santos are 3.09 Mt at 0.54%WO_3 with a cut-off of 0.1%WO_3 (Crespo *et al.* 2000) and exploitation by Heemskirk Consolidated is planned to start during 2008. The skarn is relatively poor in Mo and Sn, but locally it hosts sulfide-rich lenses with subeconomic Cu, Zn, Pb and Au grades. Los Santos now represents the second largest tungsten deposit of the Iberian Peninsula, surpassed only by Panasqueira (Portugal).

Los Santos is the only known significant tungsten-rich skarn adjacent to granodiorite in western Iberia, apart from some minor outcrops in the Spanish Central System (Casquet & Tornos 1984). However, the nearby region hosts a wide variety of tungsten mineralization, including vein- and greisen-type W–(Sn) deposits and stratabound scheelite orebodies (*e.g.*, Arribas 1979a, Derré *et al.* 1982, Pellitero *et al.* 1984). The skarn was first noted by Viladevall *et al.* (1980), but the first exhaustive study of the deposit is that of Crespo *et al.* (2000), who classified it as a reduced magnesian skarn. The existence of this orebody was interpreted as due to the magmatic-hydrothermal remobilization of earlier pre-Variscan stratiform scheelite mineralization, considered to be interbedded in the underlying metasedimentary rocks.

The main purpose of this study is to present a detailed geochemical study of the Los Santos skarn, with special emphasis on an effort to explain why the mineralization formed along an otherwise barren granodiorite–marble contact, with a test of the prevailing hypothesis that the tungsten is mobilized from a local source. The capability of scheelite for retaining high contents of Sr and REE makes it a powerful geochemical tracer. Thus, the composition of scheelite and of possible sources has been used to test the origin of tungsten and fluids.

The presence of significant amounts of REE and Sr, but minor Rb, in the structure of scheelite makes it ideal in estimating the age of the mineralization and the origin of fluids and metals (*e.g.*, Bell *et al.* 1989, Mueller *et al.* 1991, Darbyshire *et al.* 1996, Eichorn *et al.* 1997, Frei *et al.* 1998, Voicu *et al.* 2000, Kempe *et al.* 2001). Scheelite is not usually affected by super-

imposed hydrothermal (Frei *et al*. 1998) or supergene processes unless complete dissolution and reprecipitation are achieved.

Surprisingly, there are few studies dealing with the use of radiogenic isotopes in skarns. Whereas Sr isotope studies are fairly common (Van der Auwera & André 1991, Delgado *et al*. 1994), little is known on the behavior of combined Sr and Nd isotopes (*e.g*., Pan & Dong 1999). Furthermore, scheelite has been used only seldom as an isotopic tracer (Eichorn *et al*. 1997, Kempe *et al*. 2001), and usually only in orogenic gold deposits (Kent *et al*. 1995, Anglin *et al*. 1996, Frei *et al*. 1998, Voicu *et al*. 2000).

Geological Setting

The Los Santos deposit is located in the Central Iberian Zone, the internal zone of the Variscan massif of Iberia (inset in Fig. 1). Here, a metasedimentary sequence consists of a thick monotonous siliciclastic unit (Complejo Esquisto Grauvaquico) of late Neoproterozoic to early Cambrian age. It is overlain by Cambrian metasedimentary rocks. Both units, in turn, are unconformable below Ordovician siliciclastic rocks (Díez Balda 1980, Díez Balda *et al*. 1995). The Complejo Esquisto Grauvaquico can be divided into three regional units. The Lower Series (Ugidos *et al*. 1997a, b) consists of 4000–7000 m of slate, sandstone and conglomerate with turbiditic features. The unconformable Intermediate Series include about 500 m of black slate with carbonate intercalations; both the Lower and Intermediate Series are of late Neoproterozoic age. The unconformable Upper Series is dominated by sandstone and slate. On a more local scale, Díez Balda (1980) divided the Upper Series into two units. The Monterrubio Formation, of uppermost Neoproterozoic age, has about 2000 m of slate with minor intercalations of conglomerate, sandstone and volcaniclastic rocks. The conformable Aldeatejada Formation (late Vendian – early Cambrian?) consists of about 2500 m of slate with minor sandstone, limestone and debris flows. It grades into the early Cambrian Tamames Formation, 650 m thick, with interbedded fine-grained sandstone and slate deposited on a subtidal shelf. They are gradually overlain by the early Cambrian Tamames Limestone Formation (150–600 m) and capped by early to middle Cambrian Endrinal Slates. These late Paleozoic rocks are now only found in the core of E–W-trending synclines (Fig. 1).

Ugidos *et al*. (1997a, b) and Valladares *et al*. (2002) have shown that the late Proterozoic to early Cambrian slate has a distinctive geochemical signature in terms of both the whole-rock geochemistry and the Sr–Nd isotope data. Rocks of the Lower Series have a more juvenile character ($\varepsilon Nd_{545\ Ma}$ in the range –3 to –0.4), probably related to the input of sediments derived from the erosion of an immature crust. This is not observed in the Upper Series, which has a more evolved crustal signature ($\varepsilon Nd_{545\ Ma}$ in the range –7.5 to –4.4).

The Variscan architecture of the area is complex and includes widespread folding and thrusting associated with low-grade regional metamorphism (Díez Balda *et al*. 1995). Syn- to late orogenic plutonic rocks are widespread, forming the so-called Central Iberian Batholith. The earliest igneous rocks consist of two-mica granodiorite to granite, emplaced mesozonally and interpreted as synorogenic anatectic granitic rocks (Ugidos & Recio 1993). The bulk of the batholith is late orogenic and mainly made up of granodiorite to monzogranite with only minor granite *sensu stricto* (Ugidos & Recio 1993). In the study area, the dominant intrusive type consists of unoriented, usually porphyritic medium- to coarse-grained, ilmenite-bearing biotite ± cordierite granodiorite and monzogranite (the Béjar Pluton). It is cross-cut by strongly peraluminous porphyritic and fine-grained leucogranite (biotite + muscovite) and tourmaline-bearing microgranite and pegmatite (Ugidos & Recio 1993, Yenes *et al*. 1999). Geochemically, these plutonic rocks define a calc-alkaline trend (Rottura *et al*. 1989). Pinarelli & Rottura (1995) published a reference line of 318 ± 7 Ma (Rb–Sr, MSWD = 27) for the Béjar Pluton. Yenes *et al*. (1999) quoted K–Ar ages on biotite (280–270 Ma) that are younger than all of the Variscan plutonism, but contemporaneous with the onset of the Alpine Orogeny and widespread hydrothermal activity (Tornos *et al*. 2000). Thus, these K–Ar ages are probably due to partial resetting of the system. In other well-studied areas of the Spanish Central System, granodiorite and monzogranite have ages between 344 and 302 Ma, whereas the late granite have broadly younger ages, around 310–284 Ma (see Serrano Pinto *et al*. 1988, Casillas *et al*. 1991). Complex, polyphase brittle deformation with formation of strike-slip WNW–ESE faults (Yenes *et al*. 1999) was broadly synchronous with the intrusion of the granitic magmas. Granite-related hydrothermal mineralization is regionally important. There are some pegmatite and Sn-rich veins related to the synorogenic granitic rocks (Mangas & Arribas 1987, Roda Robles *et al*. 1999), but most of the mineralization is associated with small epizonal late-orogenic granite and usually consist of intra- to perigranitic W–(Sn)–quartz veins and greisen (*e.g*., Arribas 1979a, b, Mangas & Arribas 1987).

The Los Santos Skarn

The Los Santos skarn is adjacent to the WNW–ESE-trending northern intrusive contact of the Béjar Pluton (Fig. 1). The orebody is situated in a small screen of Cambrian metasedimentary rocks that correspond to the subvertical northern hinge of a southward verging syncline surrounded by the Aldeatejada Formation; the southern limb of the structure has been cut by the intrusive body (Figs. 1–3). Here, the early Cambrian

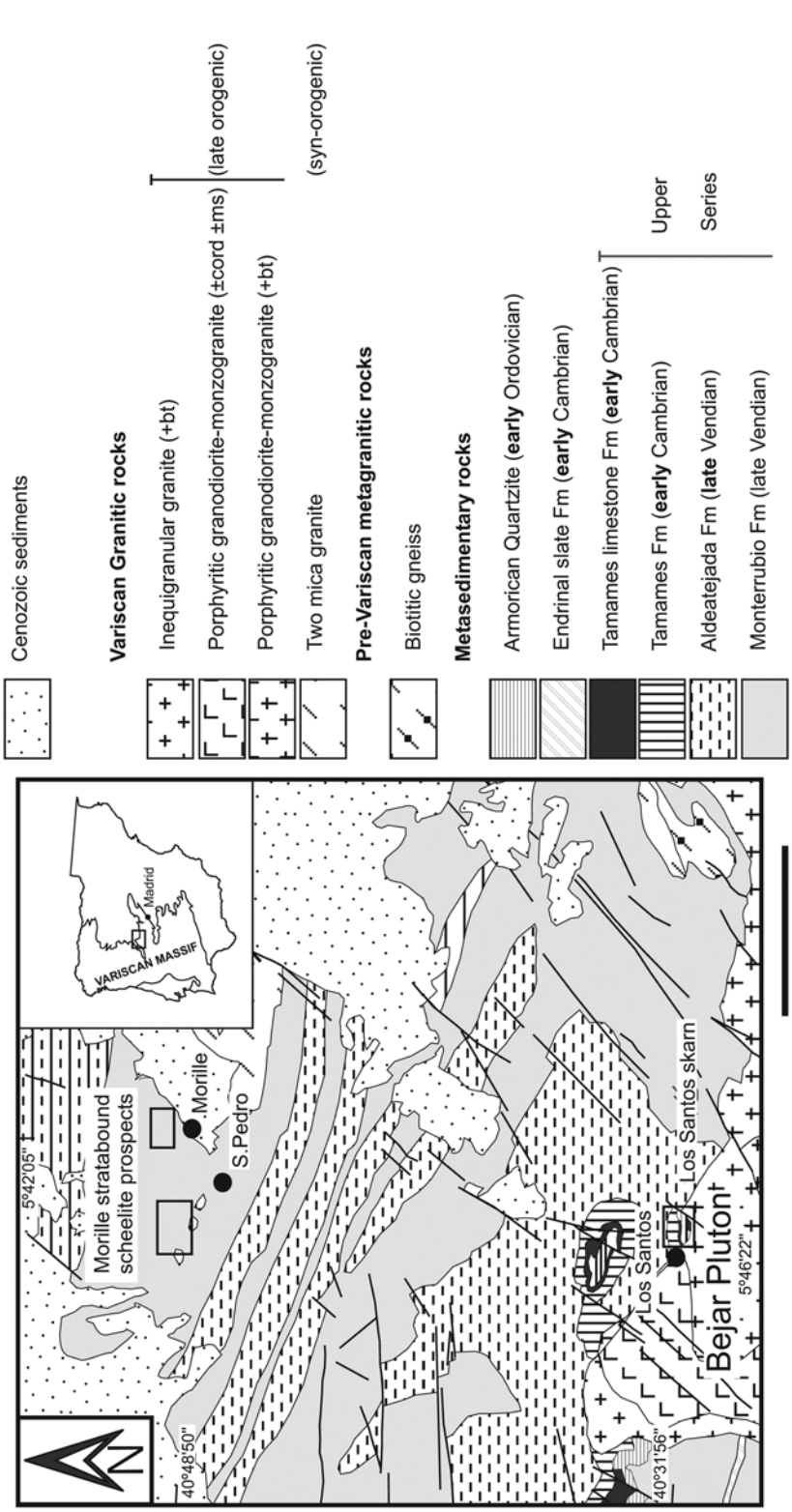

FIG. 1. Simplified geological map of the study area. Based on Diez Balda (1980), Diez Balda *et al.* (1995) and Yenes *et al.* (1999).

sequence consists of 50–200 m of limestone and dolostone interbedded with calc-silicate hornfels and siliciclastic metasedimentary rocks with sporadic pyrite-bearing black slate (*e.g.*, Díez Balda 1980). Adjacent plutonic rocks consist of oriented porphyritic biotite (+cordierite) granodiorite and monzogranite. They developed an aureole of contact metamorphism of between 1 and 8 km in width with an inner zone of K-feldspar – cordierite – biotite – andalusite – (corundum), with local development of anatexis (Timón *et al*. 2007). The highest temperature attained during contact metamorphism was about 680°C. On the basis of the contact-metamorphic assemblage, Crespo *et al*. (2000) estimated a lithostatic pressure of emplacement of about 1 kbar (100 MPa), whereas Rottura *et al*. (1989) suggested deeper conditions, near 2–3 kbar (200–300 MPa). Recent detailed work by Timón *et al*. (2007) suggests pressures of 200 to 250 MPa. These granitic rocks are in turn intruded by NE–SW-trending dikes and fault- controlled small stocks of fine-grained leucogranite. These rocks have significant amounts of andalusite, cordierite, tourmaline and relict sillimanite, and show widespread hydrothermal alteration consisting of early growth of K-feldspar of adularia habit and late conversion to white mica.

The orebody has a WNW–ESE trend and includes several lenses of mineralized skarn up to 20–30 m thick, which can be found along strike for about 2.5 km. Individual lenses are disrupted by NE–SW, N–S and NW–SE faults and leucogranite dikes (Fig. 2). The western sector consists of several aligned skarn bodies steeply dipping northward. Here, a limestone layer of about 600 m and 4–5 m thick (Capa 4) has been totally replaced by skarn. The structure is more complex in the eastern area, where the mineralization occurs in the southern limb of a SW-plunging fold (Fig. 2, Crespo *et al*. 2000).

In detail, the skarn shows a complex geometry, with irregular to stratabound exoskarn in the metasediments and an accessory massive endoskarn in the intrusive rocks (Figs. 4, 5a); the exoskarn is significantly larger by far than the endoskarn, probably in a ratio greater than 9:1. The endoskarn locally replaced an earlier greisen. This endoskarn is zoned, with a dominant plagioclase-rich skarn that is replaced by a plagioclase–pyroxene skarn and a massive pyroxenitic skarn along the contact with the marble. The contact with the granitic rocks is marked by a cm-thick zone of biotite + scheelite. The plagioclase-rich skarn is a coarse-grained massive whitish rock dominated by subhedral anorthite ($An_{91–95}$). This skarn shows gradational contacts with the plagioclase–pyroxene skarn, which includes interstitial calcic pyroxene ($Hd_{46–51}Di_{46–50}Jo_3$) that inherited the magmatic texture. (Note that compositions of the minerals are available on request from the senior author.) In both rocks, the assemblage also includes abundant scheelite and significant amounts of titanite, apatite and zircon (Fig. 5b). This zone is replaced by a massive pyroxenitic skarn, equivalent to that of the exoskarn, which masks the original intrusive contact.

The exoskarn irregularly replaced a complex sequence of interbedded impure calcitic and dolomitic marble and calc-silicate and pelitic hornfelses (Figs. 3, 4). Where the carbonate rocks are massive, the exoskarn is located only at the margin of the lenses, indicating that metasomatism was mainly controlled by fluid flow along major discontinuities. Skarn formation was especially intense where the metasedimentary sequence is lithologically heterogeneous or located directly above the plutonic rocks (Fig. 3), in a situation similar to that described in Salau (Fonteilles *et al*. 1989). In these lithologically complex rocks, discrimination of purely diffusive processes leading to the formation of skarnoids or bimetasomatic skarns (see Einaudi *et al*. 1981) or true metasomatic processes forming skarns *sensu stricto* is difficult. However, the presence of F-bearing minerals strongly suggests that even the earliest events of skarn formation involve input of external fluids and are not only due to local chemical interchange during the contact metamorphism.

The exoskarn shows a prograde zonation that is highly dependent on the composition of the protolith. In the calcitic marble, the early prograde assemblage locally consists of a cryptic zone of wollastonite followed by banded to massive grossular ($Grs_{73–76}Adr_{18–22}Sps_{5–6}$), locally abundant fluorite and minor vesuvianite. The pyroxene skarn, composed of Mn-bearing hedenbergite ($Hd_{64–83}Di_{6–31}Jo_{4–14}$), shows complex relationships with the garnet-rich one (Figs. 5c, d). They show evidence of mutual replacement; however, the broad distribution of the pyroxene skarn closer to the endoskarn suggests that it formed dominantly as a replacement of an earlier garnet-rich zone. There is a second generation of zoned anisotropic granditic garnet ($Grs_{43–71}Adr_{24–29}Sps_{4–27}$) in veins or masses cross-cutting the earlier pyroxene or garnet skarn.

The exoskarn developed in the calc-silicate and pelitic hornfelses (periskarn) shows a similar sequence, with an early fine-grained clinopyroxene replaced by the coarse-grained Mn-rich hedenbergite, granditic garnet and vesuvianite. The calcic exoskarn is rich in coarse-grained, Mo-poor (0.1–0.2% MoO_3) scheelite, apatite and titanite (Fig. 5e).

In the dolomitic marble, the metasomatic sequence starts with a complex fine-grained magnesian skarn with forsterite ($Fo_{85–98}$), diopside, minerals of chondrodite group, phlogopite, spinel–hercynite and magnetite (Crespo *et al*. 2000, Timón *et al*. 2007), which is replaced by a characteristic fine-grained diopside zone, grossular-rich garnet and the pyroxene skarn. No mineralization has been observed in the magnesian exoskarn. This evolution is similar to that observed in equivalent settings, in which an initial magnesian skarn is replaced by a calcic and scheelite-bearing variety

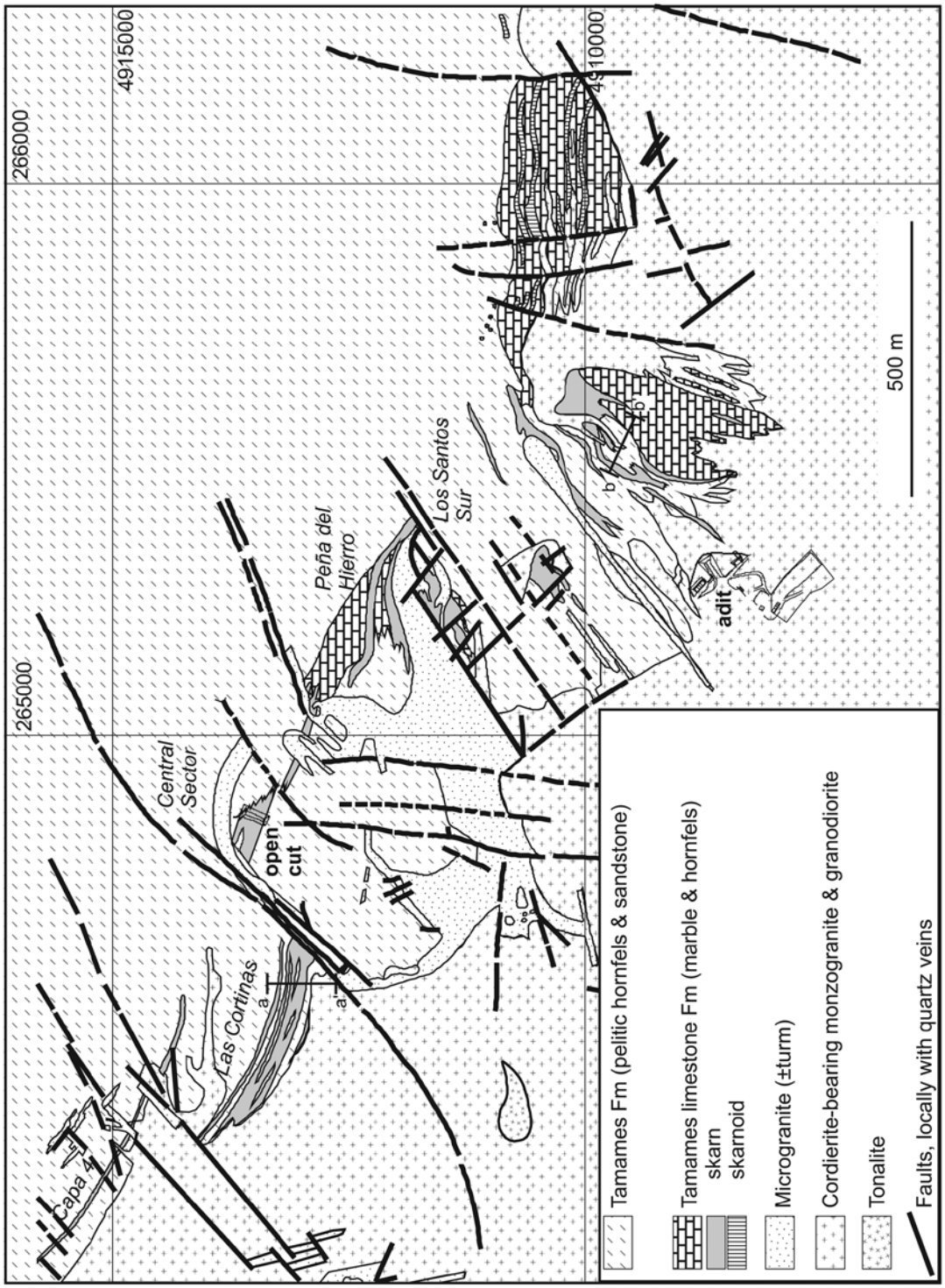

FIG. 2. Geological map of the Los Santos skarn. The cross sections of Figure 3 are shown as a–a' and b–b'. Modified from SIEMCALSA.

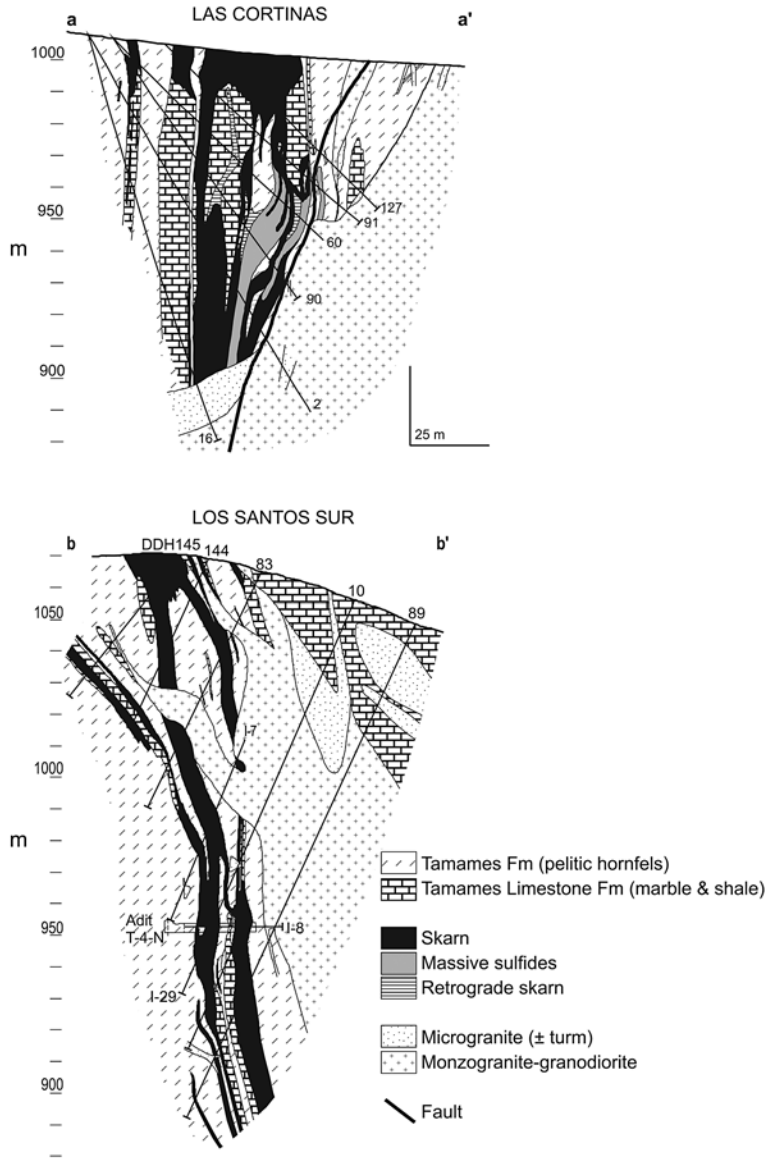

FIG. 3. Selected detailed cross-sections of the Los Santos skarn in the Las Cortinas and Los Santos Sur areas (Fig. 2). Modified from SIEMCALSA.

(*e.g.*, Costabonne: Guy 1979, Carro del Diablo: Casquet & Tornos 1984).

The retrograde skarn (or aposkarn) is volumetrically minor and has an irregular distribution. It discordantly replaced both the endo- and exoskarn along lithological contacts and minor faults. It is dominated by clino-amphibole (magnesiohornblende and ferrohornblende, ferro-edenite and ferro-actinolite), K-feldspar, quartz, calcite, scheelite and accessory epidote; scapolite is locally abundant. In general, the amphibole replaced the hedenbergite and the early grossular, whereas the late granditic garnet seems to have been stable during the formation of the retrograde skarn. Locally, there is a biotite-rich skarn replacing the pelitic hornfels. It is composed of coarse-grained, locally oriented biotite with interstitial quartz, abundant scheelite and apatite (Fig. 5f). These biotite-rich and strongly mineralized facies are similar to those described by Cheilletz

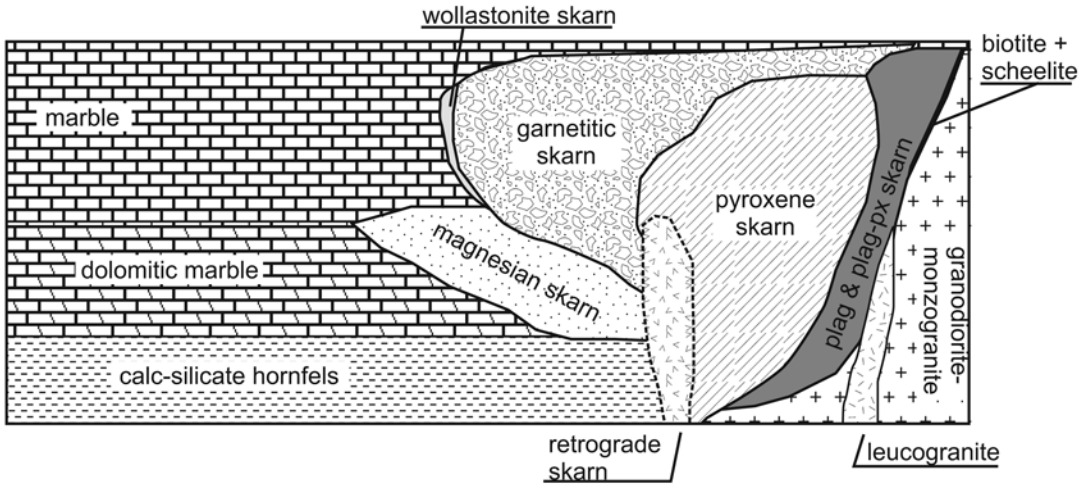

FIG. 4. Geological sketch illustrating skarn zonation in the granodiorite–monzogranite contact with the Tamames Limestone Formation.

(1985) and Giuliani *et al*. (1987) at Djebel Aouman (Morocco).

The magnesian skarn is replaced by tremolite, clintonite, and serpentine. Finally, there are late veins and replacements of quartz, K-feldspar of adularia habit, ferroan clinochlore, calcite, epidote, fluorite, apatite and prehnite. Locally, there are massive veins of talc, apatite and scheelite.

Despite some scheelite in the retrograde skarn, about 80% of the tungsten mineralization is located in the pyroxene skarn. In general, the skarn is sulfur-poor, with the sulfides restricted to irregular lenses up to 8–10 m thick and 50 m long, amounting to 0.25 Mt, replacing marble, calc-silicate hornfels or the prograde skarn (Fig. 5g). These lenses consist of semimassive pyrrhotite and pyrite with minor chalcopyrite, galena and arsenopyrite–löllingite, Fe-bearing sphalerite (6–12 wt% Fe), bismuthinite (partially retrograded to native bismuth), Bi–Ag–Te sulfosalts and minor ferberite intergrown with quartz and carbonates. They are tungsten-rich (1–2% WO_3), and local appreciable gold grades have been recorded. The tin content is invariably low (<100 ppm; Crespo *et al*. 2000).

THE STRATIFORM SCHEELITE MINERALIZATION: MORILLE MINES

Near the Los Santos deposit, stratiform scheelite mineralization can be found as abundant, small lenses within the Monterrubio Formation (Fig. 1). The scheelite is hosted by calc-silicate hornfels replaced by a calcic skarn (skarnoid) within a sequence including quartzite, amphibolite, schist and quartz–feldspar and plagioclase–biotite gneiss (Arribas 1979a), without adjacent granitic rocks. The skarnoid shows the typical bimetasomatic zoning of reaction skarns, developed along the contact between calcic and aluminum-rich rocks. It consists of complex massive to banded coarse aggregates of quartz, biotite, plagioclase, diopsidic pyroxene, granditic garnet, phlogopite, scapolite or pargasitic clinoamphibole, which locally host an inner zone with anorthite, granditic garnet and vesuvianite (Fig. 5h). In some places, the core of these lenses is made of calcite, suggesting that these rocks could replace original calcitic marble; accessory scheelite,

FIG. 5. Photographs showing relevant aspects of the Los Santos orebody. (a) Intrusive contact between the granodiorite–monzogranite totally replaced by plagioclase-rich endoskarn with pyroxene and garnet skarn. (b) Photomicrograph of the plagioclase skarn, formed by subhedral crystals of anorthite with clinopyroxene (cpx), abundant scheelite (sch) and titanite (tt). Plane-polarized transmitted light, width of field of view: 3 mm. (c) Aspect of the prograde skarn replacing marble (cc) with relict garnet skarn (gr) almost totally replaced by pyroxene skarn (px). (d) Pyroxene skarn (px) replaced by garnet skarn (gr). (e) High-grade pyroxene skarn with coarse crystals of hedenbergite (px) and abundant interstitial scheelite (sch) and some titanite (tt). Plane-polarized transmitted light, width of field of view: 3 mm. (f) Microscopic aspect of the biotite-rich skarn with oriented bands of biotite and quartz and abundant scheelite (sch) and apatite. Plane-polarized transmitted light, width of field of view: 3 mm. (g) Massive sulfides replacing calc-silicate hornfels. (h) Banded distal skarn with calc-silicate-rich layers (plagioclase, quartz, pargasite, diopside and scheelite) interbedded with pelitic schist. Morille.

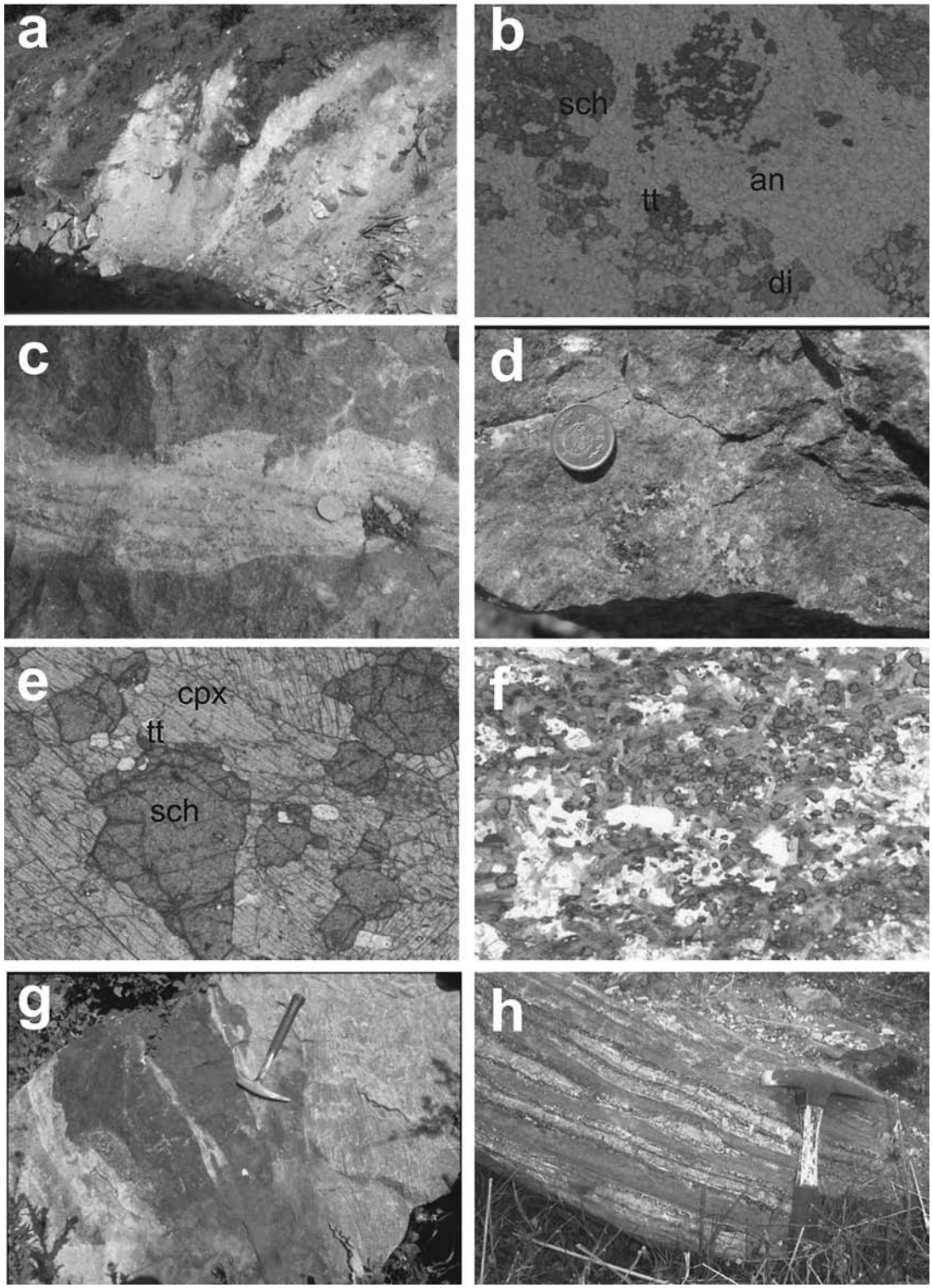
a
b
sch
an
tt
di
c
d
e
cpx
tt
sch
f
g
h

titanite and malayaite are disseminated in the skarnoid. There is a late assemblage with epidote, chlorite and white mica. This mineralization is broadly similar to many other minor skarn-like orebodies found in northern Iberia and hosted by Proterozoic (Arribas 1979a) and Ordovician–Silurian sedimentary sequences (Derré *et al.* 1982, Arribas 1983, Pinto 1986).

Arribas (1979a) originally suggested that the tungsten mineralization is pre-Variscan in origin and probably corresponds to metamorphosed exhalative orebodies with only local remobilization. Pellitero *et al.* (1984) proposed that the scheelite was deposited during the Variscan regional metamorphism, with hydrothermal leaching of tungsten from the host sequence and further reconcentration in the calcic-rich rocks. In other areas, geological and geochemical studies indicate a direct genetic relationship between granites and this type of mineralization, suggesting that they are distal perigranitic skarns (Derré *et al.* 1982, Pinto 1986, Casquet & Tornos 1991, Gaspar & Inverno 2000). The same debate about the origin of stratabound scheelite mineralization in metamorphic belts is found elsewhere (see Einaudi *et al.* 1981, Kwak 1987).

The Perigranitic Veins of La Parrilla

Perigranitic tungsten-bearing veins are widespread in the Variscan Belt of Iberia (see Tornos & Gumiel 1992). Perhaps one of the most representative and best studied deposits is La Parrilla, located about 90 km south of Los Santos, but formed in an equivalent setting within the lowermost Complejo Esquisto Grauváquico (Gumiel & Pineda 1981, Mangas & Arribas 1988). Here, NE-trending veins bearing scheelite, cassiterite and arsenopyrite–quartz cross-cut pelitic hornfels with intense contact metamorphism produced by an underlying late Variscan epizonal granite.

Analytical Methods

Samples were crushed, and the minerals were separated by handpicking after a thorough petrographic study. Owing to the small grain-size, scheelite samples of Los Santos and Morille were obtained from ore concentrates, whereas the scheelite of La Parrilla was hand-picked from coarse grains in the veins. Stable isotope analyses were performed at the NERC Isotope Geoscience Laboratory (British Geological Survey). Silicate samples (10–15 mg) were prefluorinated with ClF_3 at room temperature and then were reacted with a stoichiometric excess of ClF_3 at 650°C for 12 hours (Borthwick & Harmon 1982, Venneman & Smith 1990). The oxygen released was converted to CO_2 by reaction with a hot platinum-coated graphite rod (Clayton & Mayeda 1963). The isotope ratio was measured with a modified VG 9037 gas-source mass spectrometer. Commercial CO_2 was used as reference gas calibrated against laboratory standards. Oxygen isotope results are reported in δ-notation relative to SMOW. Standard NBS–28 gave 9.6 ± 0.0‰ SMOW. The overall analytical reproducibility is better than ±0.2‰.

Strontium and Nd radiogenic isotope analyses were carried at the CAI de Geocronología y Geoquímica Isotópica, Universidad Complutense de Madrid. Scheelite was decomposed in cold hydrochloric acid in SAVILLEX7 teflon vessels placed in an ultrasonic bath. The ultrasonic treatment removes the protective coating of tungstic acid from the scheelite grains, thus allowing complete dissolution. The solutions were centrifuged and decanted from the insoluble tungstic acid residue. Strontium and the rare-earth elements (REE) were separated from the solution by conventional ion-exchange techniques (DOVEX AG–507® resin). Strontium was loaded on single tantalum filaments prepared with 1 μm of 1 M phosphoric acid. Neodymium was separated from the bulk REE fraction on a column filled with Biobeads7 coated with bis di-ethylhexyl hydrogen phosphate (HPEHP). Samples were loaded with 1 mL of 0.05 M phosphoric acid on tantalum side filaments of a triple filament assembly with a rhenium filament in the center. Isotopic analyses were made on an automated multicollector VG Sector-547 mass spectrometer. Errors are quoted throughout as two standard deviations from measured values. Replicate analyses of the NBS–987 Sr isotope standard yielded an average $^{87}Sr/^{86}Sr$ value of 0.710256 ± 0.000008 (n = 7), and analyses of La Jolla Nd standard during 2000 gave a mean $^{143}Nd/^{144}Nd$ value of 0.511858 ± 0.00003 (2σ). Total uncertainties are estimated to be 0.01% for $^{87}Sr/^{86}Sr$, 0.006% for $^{143}Nd/^{144}Nd$, 1.0% for $^{87}Rb/^{86}Sr$ and 0.1% for $^{147}Sm/^{144}Nd$. Rubidium, strontium, molybdenum, and rare-earth concentrations were obtained by ICP–MS at the University of Granada. Strontium and Nd isotope values for the host rocks have been published by Ugidos *et al.* (1997a) and Pinarelli & Rottura (1995). Complementary analyses of the leucogranite dikes near the mineralization are also presented in Table 1.

For the calculations, an average age of formation of 300 Ma has been assumed. As discussed above, this is a reasonable average age of intrusion of granitic magmas in the Spanish Central System. Variations in the isotopic ratio due to the true age of intrusion and ore-forming process (between 340 and 280 Ma) do not noticeably modify the conclusions (see Pinarelli & Rottura 1995, Timón *et al.* 2007).

The fluid-inclusion and thermodynamic constraints presented by Timón *et al.* (2007) indicate that the formation of the prograde skarn took place owing to the circulation of saline (7.6–9.8 wt% NaCl eq.) H_2O-rich fluids [$X(H_2O) = 0.95$] with minor proportions of CO_2 and traces of CH_4 and N_2 at temperatures between 550 and 680ºC. This range of temperature is consistent with that of similar prograde assemblages in the Spanish Central System (Tornos *et al.* 2000) and elsewhere (see Einaudi *et al.* 1981, Kwak 1987, Meinert *et al.* 2005, and references therein). There are no data about

the minor late skarn, but they usually occur in the 300–400°C range.

Stable Isotopes

The $\delta^{18}O$ composition of both granditic garnet and pyroxene of the early skarn is very homogeneous, 7.8–7.9‰ and 7.5–8.4‰, respectively (Table 2). This isotope signature should be a function of the reaction of the host limestone with an inflowing fluid in chemical and isotopic disequilibrium. A simple numerical estimation using the data on the solubility of silica (Walther & Helgeson 1977) at 2 kbar shows that at 550–600°C, the fluid:rock ratio needed to form massive hedenbergite- and granditic-garnet-rich skarns by replacement of a limestone by a Si–Fe-bearing fluid exceeds 50000 (by weight); this proportion must be significantly greater if a kinetic effect is taken into account. These figures are consistent with the isotope data presented by Rose *et al.* (1985), Bowman (1998), Wang & Williams (2001) and Zürcher *et al.* (2001), who showed that the isotopic composition of the skarn silicates is usually constrained by the inflowing fluid; the amount of oxygen inherited from the protolith is negligible. Even in silica-rich impure carbonatic rocks, as those found at Los Santos, the $\delta^{18}O$ isotopic shift due to metamorphic decarbonation (distillation) processes is minimal when compared to that imposed by the large amount of oxygen added by the external fluids.

Thus, the best approximation to the isotopic composition of the hydrothermal fluid can be estimated from the $\delta^{18}O$ values of the skarn minerals at 550–680°C with the $\delta^{18}O_{mineral-H_2O}$ of Zheng (1993), which yields values between 9.5 and 10.9‰. The data show that these minerals grew in isotopic equilibrium and from a fluid strongly enriched in ^{18}O, with no significant varia-

TABLE 1. TRACE-ELEMENT AND RADIOGENIC ISOTOPE DATA ON SCHEELITE, SKARN AND LEUCOGRANITE

	Scheelite								Plagioclase sk	
Sample	AL-3	AL-3-1	LS-29	LS-30	LS-31	LS-57	LP-1	LP-2	LS-62	LS-63
Locality	M	M	LS	LS	LS	LS	LP	LP	LS	LS
Rb ppm	0.8	1.1	0.2	0.2	0.2	0.7	0.5	0.7	<2	<2
Sr	2019	1813	105	83	94	109	39	40	319	242
Mo	3	8	102	91		99	0	0		
Cu	5	<3	125	33		103	8	88		
Zn	<1	2	117	33		39	5	43		
Pb	1	4	4	7		2	1	1		
Sn	67	64	2	2		3	2	1		
La	5.0	6.2	35.6	54.2		39.0	21.8	24.7	3.9	6.8
Ce	14.6	16.0	95.1	136.6		104.9	41.4	48.9	7.6	9.4
Pr	1.7	1.9	12.9	18.3		14.4	5.3	6.2	1.0	1.3
Nd	7.0	9.0	54.0	76.0	54.2	61.8	24.7	27.6	4.7	6.5
Sm	2.2	2.7	10.9	15.7	13.3	12.0	7.7	8.7	<1.6	1.8
Eu	0.9	2.6	1.3	1.6		1.3	23.9	26.9	<0.3	<0.3
Gd	2.6	3.0	9.3	13.0		10.0	10.8	11.8	<1.6	1.7
Tb	0.5	0.6	1.2	1.8		1.4	2.3	2.5	<0.3	<0.3
Dy	3.1	3.8	6.1	9.5		6.9	17.8	18.6	1.4	1.8
Ho	0.7	0.9	1.2	1.9		1.3	4.2	4.5	<0.3	<0.3
Er	2.1	2.7	2.8	4.7		2.9	13.6	14.2	0.8	1.0
Tm	0.4	0.5	0.3	0.7		0.4	2.4	2.5	<0.3	<0.3
Yb	2.4	3.0	1.6	3.5		1.8	16.7	17.7	1.0	1.2
Lu	0.4	0.5	0.2	0.5		0.2	2.4	2.6	<0.3	<0.3
ΣREE	44	53	233	338		258	195	217	20	31
$[La/Yb]_N$	1.4	1.4	15.1	10.6		14.8	0.9	1.0	2.8	3.9
Eu/Eu*	0.77	1.92	0.27	0.23		0.24	5.65	5.70		
$^{87}Rb/^{86}Sr$	0.0011	0.0018	0.0276	0.0347	0.0308	0.0174	0.0459		0.0091	0.0120
$^{87}Sr/^{86}Sr$	0.710828	0.710984	0.711955	0.711850	0.711908	0.712017	0.714955		0.712404	0.713000
$^{87}Sr/^{66}Sr_i$	0.7108	0.7110	0.7118	0.7117	0.7118	0.7119	0.7148		0.7124	0.7129
$^{147}Sm/^{144}Nd$	0.1836	0.1820	0.1218	0.1249	0.1482	0.1175	0.1897		0.2572	0.1674
$^{143}Nd/^{144}Nd$	0.512170	0.512170	0.512051	0.512057	0.512065	0.512047	0.512394		0.512260	0.512223
$^{143}Nd/^{144}Nd_i$	0.5118	0.5118	0.5118	0.5118	0.5118	0.5118	0.5120		0.5118	0.5119
εNd_{300}	-8.7	-8.6	-8.6	-8.6	-9.4	-8.5	-4.5		-9.7	-7

Legend: M: Morille, LS: Los Santos, LP: La Parrilla. The samples were analyzed for the rare-earth elements at the Department of Petrology, Granada University and IGME. They were analyzed for radiogenic isotopes at the Laboratory of Geochonology and Isotope Geology, Universidad Complutense Madrid.

TABLE 1 (cont'd). TRACE-ELEMENT AND RADIOGENIC ISOTOPE DATA OF SCHEELITE, SKARN AND LEUCOGRANITE

	Pyroxene skarn		Leucogranite		Marble		CS Hornfels	Pelitic hornfels	
	LS-64 LS	LS-65 LS	LS-55 LS	LS-56 LS	LS-60 LS	LS-61 LS	LS-66 LS	LS-68 LS	LS-72 LS
Rb ppm	<2	<2	368.1	282.6	<2	<2	<2	78.0	21.0
Sr	44	37	18	43	437	416	707	76	70
Mo			1	4					
Cu			4	7					
Zn			25	12					
Pb			28	27					
Sn			12	10					
La	3.0	13.8	2.3	3.2	3.7	2.3	39.8	42.8	24.7
Ce	6.1	24.5	4.3	5.8	7.4	4.6	80.3	79.3	44.0
Pr	0.7	2.6	0.5	0.6	0.9	0.5	9.1	9.3	5.3
Nd	3.7	10.7	2.2	2.8	4.5	3.2	32.8	35.6	18.0
Sm	<1.6	1.8	0.5	0.6	<1.6	<1.6	6.6	7.1	4.2
Eu	<0.3	0.5	0.1	0.2	<0.3	<0.3	<0.3	1.2	<0.3
Gd	0.9	1.6	0.6	0.5	<1.6	<1.6	5.5	5.9	3.7
Tb	<0.3	<0.3	0.1	0.1	<0.3	<0.3	0.6	0.7	0.4
Dy	0.9	1.3	0.7	0.2	0.7	0.5	4.3	4.8	3.0
Ho	<0.3	<0.3	0.1	0.0	<0.3	<0.3	0.7	0.9	0.5
Er	0.6	0.9	0.4	0.3	0.3	<0.3	2.2	2.7	1.8
Tm	<0.3	<0.3	0.1	0.1	<0.3	<0.3	<0.3	<0.3	<0.3
Yb	1.0	0.8	0.4	0.5	0.4	<0.3	2.1	2.5	1.6
Lu	<0.3	<0.3	0.1	0.1	<0.3	<0.3	<0.3	<0.3	<0.3
ΣREE	17	59	12	15	18	11	184	193	107
$[La/Yb]_N$	2.1	12.0	3.7	4.5	6.8		13.1	11.9	10.7
Eu/Eu*		0.64	0.40	0.72				0.38	
$^{87}Rb/^{86}Sr$	0.0658	0.0782	60.7918	19.0673	0.0066	0.0070	0.0041	2.9757	0.8694
$^{87}Sr/^{86}Sr$	0.713128	0.712264	0.970744	0.796325	0.709637	0.709685	0.712405	0.729346	0.724415
$^{87}Sr/^{86}Sr_i$	0.7128	0.7119	0.7112	0.7149	0.7096	0.7097	0.7124	0.7166	0.7207
$^{147}Sm/^{144}Nd$	0.1634	0.1017	0.1321	0.1354			0.1216	0.1206	0.1410
$^{143}Nd/^{144}Nd$	0.512137	0.512007	0.512278	0.512231			0.512026	0.512033	0.512066
$^{143}Nd/^{144}Nd_i$	0.5118	0.5118	0.5120	0.5120			0.5118	0.5118	0.5118
εNd_{300}	-8.5	-8.7	-4.6	-5.6			-9.1	-8.9	-9.1

CS Hornfels: calc-silicate hornfels. LS: Los Santos.

tions of its isotopic composition with time. The silicate minerals of the retrograde skarn show similar values. Their stable isotopic compositions suggest $\delta^{18}O_{fluid}$ values between 9.1 and 11.3‰. Within the margin of error, these compositions are equivalent to those of the early skarn. Again, it is unlikely that the retrograde skarn inherited the oxygen isotope signature from the prograde one (*e.g.*, Bowman 1998). This strongly suggests that the formation of the whole skarn is related to a single, probably long-lived hydrothermal event, and that the hydrothermal fluids were either derived from a homogeneous source or were completely homogenized during fluid circulation. Neither the exact temperature of formation nor the influence of the granditic garnet and hedenbergite–diopside solid solutions are critical, because the $\Delta^{18}O_{mineral-fluid}$ does not change significantly within the assumed range of values (<1‰).

The calcite intergrown with the amphibole of the retrograde skarn yields a wide range of values, but imply $\delta^{18}O_{fluid}$ signatures of 6.2 to 15.4‰ (Table 3). The limestone adjacent to the wollastonite skarn (samples LS–53a and b) has similar isotopic signatures. These signatures (12.8–12.9‰) are within the range of Cambrian limestone affected by late diagenetic processes in other areas of the Iberian Peninsula ($\delta^{18}O$: 10.5 to 16‰; $\delta^{13}C$: –4.6 to 1.5‰), but are also similar to those of the retrograde skarn. Thus, they either represent the pre-skarn isotopic composition of the limestone or indicate that fluids associated with the retrograde skarn formed a halo external to the skarn and were able to reset the limestone's isotopic values. A similar situation with isotopic fronts preceding chemical reaction fronts has been described by Blattner & Lassey (1989). The calculated $\delta^{13}C_{fluid}$ signatures (–5 to 0‰) are consistent with derivation of the carbon for the carbonates from the host limestone, perhaps with a minor influence of a ^{12}C-enriched carbon derived from the underlying metapelitic rocks (see below).

The consistently heavy isotopic $\delta^{18}O$ signature of calc-silicates supports a derivation from magmatic or

metamorphic sources, as discussed by Sheppard (1986), and preclude any significant input of marine or meteoric surficial fluids. The host granites have $\delta^{18}O$ signatures near 8.0 to 10.3‰ (Recio *et al.* 1992), whereas the slate has $\delta^{18}O$ values between 9.3 and 13.8‰ (Recio *et al.* 1992, Ugidos *et al.* 1997a). Fluids in equilibrium with these rocks at magmatic and contact-metamorphic temperatures (>500°C) would have signatures above 9.2‰, in close agreement with the observed values. Surficial fluids with initial $\delta^{18}O$ values below 0‰ could certainly also attain heavy $\delta^{18}O$ signatures if they became completely equilibrated with the host rocks at temperatures above 300–350°C. Such a high degree of chemical equilibration would imply fluids isotopically indistinguishable from deep fluids, an alternative that seems very unlikely. Surficial fluids that flowed deeply within the crust in other areas of the Spanish Central System usually retain low $\delta^{18}O$ values (<5‰; Tornos *et al.* 2000), indicating only partial equilibration with the basement.

The REE Geochemistry of the Scheelite and Associated Minerals

The REE content of skarn minerals (except Eu) replacing marble at hydrothermal temperatures and high fluid:rock ratio is mainly controlled by the incoming fluid and the partition coefficients (K_D) of the paragenetic minerals with the fluid; synchronous precipitation of garnet, monazite, zircon and apatite can dramatically influence their relative REE contents, but their exact control cannot be evaluated. The REE of the replaced marble has little effect, as concentrations are very low (*e.g.*, Gieré 1986, Van der Auwera & André 1991; see also Table 1). The K_D values for many skarn minerals are unknown and, thus, little can be said about the composition of fluids (Ghaderi *et al.* 1999, Kempe *et al.* 2001). However, Pan & Fleet (1992) and Giuliani *et al.* (1987) suggested that the effect of the K_D is perhaps not so significant and that the REE profile of hydrothermal minerals is inherited from the hydrothermal fluid.

As quoted above, scheelite concentrates the REE; in theory, it should thus behave as a good tracer for fluid–rock interaction. However, Ghaderi *et al.* (1999) have shown that the model is complex; in addition to the parameters discussed above, the partitioning of REE between scheelite and hydrothermal fluids is highly dependent on crystal-structure and charge-balance aspects. The existing data show that the REE contents of scheelite definitely vary according to the type of deposit. In fact, REE profiles from Los Santos and Djebel Auman (Giuliani *et al.* 1987), with seagull-like shapes, are dramatically different from those of orogenic gold deposits (Anglin *et al.* 1996, Ghaderi *et al.* 1999, Oberthur *et al.* 2000, Kempe *et al.* 2001), usually characterized by a dome-like shape.

The scheelite from the deposits studied here has low ΣREE and Sm–Nd concentrations compared to scheelite in other skarns (Giuliani *et al.* 1987) and, indeed, other mineral deposits (*e.g.*, Darbyshire *et al.* 1996, Voicu *et al.* 2000). Figure 6 shows the REE profiles of our scheelite, skarn and adjacent rocks, including metasedimentary rocks, leucogranite (Table 1) and granodiorite–monzogranite (Pinarelli & Rottura 1995). The La Parrilla and Morille scheelite has almost flat profiles ($0.3 < [La/Yb]_N < 1.8$). The REE content of the scheelite in the Morille mineralized zone is low (ΣREE in the range 44–53 ppm), and the REE profiles show a small positive Eu anomaly (Eu/Eu* in the range 0.3–0.6). The scheelite from La Parrilla has slightly higher ΣREE contents (195–218 ppm) and a positive Eu/Eu* value, 1.8. Scheelite from Los Santos has the highest ΣREE contents (233–338 ppm), a marked negative Eu anomaly (Eu/Eu* = 0.1) and values of $[La/Yb]_N$ between 10.6 and 15.1. The other group of samples includes the metasedimentary rocks and the granodiorite–monzogranite, all of them showing a characteristic depletion in HREE and a seagull-like pattern, with high $[La/Yb]_N$ values, greater than 10. The metasedimentary rocks (other than the marble, which has low REE contents) have average ΣREE of 200 ppm with Eu/Eu* equal to 0.13, whereas the granodiorite–monzogranite averages 170 ppm ΣREE, with a Eu/Eu* of 0.38. Finally, the leucogranite and the skarn have intermediate [La/Yb]

TABLE 2. STABLE ISOTOPE COMPOSITION OF SILICATES

Sample	Rock	Mineral	$\delta^{18}O$	T°C	$\delta^{18}O_{fluid}$
LS-54a	Pyroxenitic exoskarn	Hedenbergite	7.5	550-680	9.5-9.6
LS-54b	Pyroxenitic exoskarn	Hedenbergite	7.5	550-680	9.5-9.6
LS-A	Pyroxenitic exoskarn	Hedenbergite	7.9	550-680	9.9-10.0
LS-17	Pyroxenitic exoskarn	Hedenbergite	8.4	550-680	10.4-10.5
LS-A	Garnetitic exoskarn	Grandite	7.9	550-680	10.8-10.9
LS-B	Garnetitic exoskarn	Grandite	7.8	550-680	10.7-10.8
LS-28	Late exoskarn	Biotite	8.6	300-400	11.3
LS-21	Late exoskarn	Biotite	6.4	300-400	9.1
LS-22	Late exoskarn	Biotite	7.4	300-400	10.1
LS-51	Late exoskarn	Ferro-actinolite	9.3	300-400	10.6-12.0
LS-50a	Late exoskarn	Ferro-actinolite	9	300-400	10.3-10.6
LS-50b	Late exoskarn	Ferro-actinolite	9.2	300-400	10.5-10.8

Fractionation factors: clinopyroxene-H_2O, as hedenbergite; garnet-H_2O, as grossular; biotite-H_2O and ferro-actinolite-H_2O: Zheng (1993). Analysis NIGL. The values of $\delta^{18}O$ are expressed in ‰.

TABLE 3. STABLE ISOTOPE COMPOSITION OF CARBONATES

Sample	Description	Mineral	$\delta^{18}O$	$\delta^{13}C$	T°C	$\delta^{18}O_{fluid}$	$\delta^{13}C_{fluid}$
LS-33	Calcite amphibole skarn	Calcite	11.8	-6.9	400	8.5	-4.5
LS-34	Calcite amphibole skarn	Calcite	12.3	-2.8	400	9.1	-0.5
LS-49	Calcite amphibole skarn	Calcite	12.8	-6.1	400	9.5	-3.8
LS-53a	Host limestone	Calcite	12.9	-5	400	9.6	-2.7
LS-53b	Host limestone	Calcite	12.8	-5	400	9.6	-2.7

Analysis NIGL. Fractionation factors from Friedman & O'Neil (1977). The values of $\delta^{18}O$ and $\delta^{13}C$ are quoted in ‰.

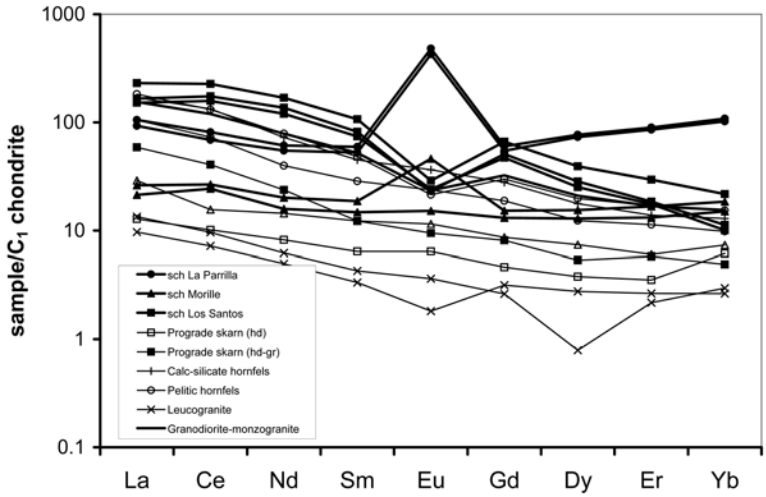

FIG. 6. Rare-earth profiles of the scheelite and host rocks, normalized to chondrite. The REE profile of the host granodiorite–monzogranite is the average of values from Pinarelli & Rottura (1995). Marble and plagioclase skarn LS–62 have HREE contents close or below the detection limit and are not shown. In the other samples, the REE contents below detection limit are extrapolated by averaging contiguous elements. Symbols: sch: scheelite; wr: whole rock.

$_N$ values. The plagioclase skarn has $[La/Yb]_N$ values of 2.8 and 3.9, whereas in the prograde skarn, the $[La/Yb]_N$ values are very variable, low in the hedenbergite skarn (2.1) and significantly higher where it has garnet (12). This depletion in HREE strongly suggests that the skarn-related garnet (see also Smith *et al.* 2004) does not incorporate large amounts of REE, as does garnet of magmatic origin. Both magmatic garnet and pyroxene show an affinity for the HREE and typically show a negative Eu anomaly (Hanson 1980).

The leucogranite has low REE contents (12–15 ppm) and an irregular REE pattern, with no Eu anomaly ($3.7 < [La/Yb]_N < 4.8$, $0.1 < Eu/Eu^* < 0.3$). The REE profile of the granodiorite–monzogranite is similar to that of the granitic rocks of the Spanish Central System. These rocks show a seagull pattern, with a negative Eu anomaly that increases gradually from the more basic rocks to the leucogranite (Casillas *et al.* 1991). This pattern is typical of reduced plutonic rocks (Hanson 1980), with progressively more crustal influence and zircon crystallization depleting the HREE from the fluid (Cullers & Graf 1984, Nie 1994). The LREE are relatively incompatible in magmatic minerals, and thus are enriched in the residual melt. Thus, evolved leucogranite and exsolved magmatic-hydrothermal fluids usually have a seagull-like pattern (Cullers & Graf 1984, Darbyshire & Shepherd 1985). The absence of such a negative Eu anomaly in the Los Santos leucogranite (Fig. 6) can only be attributed to the existence of a superimposed pervasive hydrothermal alteration. Divalent Eu is not accommodated in the structure of a white mica, and thus, the conversion of plagioclase to white mica releases Eu^{2+} to the hydrothermal fluids. Poitrasson *et al.* (1995) have described the leaching of Eu and concomitant dilution of the Eu negative anomaly by reaction of F-rich fluids with granite.

If the K_D rock–fluid in the different rocks is assumed to be broadly similar, the zonation leucogranite – plagioclase skarn – prograde skarn can be explained as due to the progressive interaction of a REE-depleted leucogranite-equilibrated fluid with the REE-rich granodiorite–monzogranite or hornfels. In detail, the size of the Eu anomaly in scheelite is controlled by the Eu content and the Eu/Eu* value of the fluid as well as the presence of sites suitable for Eu substitution in the structure of scheelite (Ghaderi *et al.* 1999). The Eu_N *versus* Eu^*_N relations strongly suggest that scheelite from the Los Santos deposit precipitated from a fluid with some of the Eu occurring in the trivalent form. The available results align along trends parallel to the 1:1 ratio and have intermediate Eu_N and Eu^*_N values that are consistent with such an oxidation state (Ghaderi *et al.* 1999). In this case, the negative Eu anomaly is derived from the fluid, suggesting that the hydrothermal fluids were impoverished in Eu.

Accordingly, the scheelite from La Parrilla seems also to be formed from fluids carrying some Eu as Eu^{3+}, but its profile is more consistent with derivation

from the hydrothermal alteration of granite. The HREE enrichment is interpreted as due to the hydrothermal leaching of zircon, xenotime and other similar phases during extreme hydrothermal alteration. In this context, the Eu/Eu* value could indicate that hydrothermal fluids have inherited their Eu from the destruction of plagioclase. The profile of scheelite from Morille is less clear; the high Eu/Eu* values are misleading because they can be related to reduced fluids or to fluids that have an inherited Eu anomaly (Ghaderi *et al*. 1999).

Radiogenic Isotope Results: the Source of Sr and Nd

The Sr and Nd isotope geochemistry of the scheelite, skarn and the host rocks provide significant insights into the source and evolution of fluids (Fig. 7). The low Nd content of the marble (<5 ppm; Table 1) implies that almost all the Nd of the scheelite must have been derived from external fluids or adjacent rocks. The granitic rocks of the Béjar Pluton have typical crustal values ($\varepsilon Nd_{300\ Ma} = -5.9 \pm 1.4$; $^{143}Nd/^{144}Nd_{300\ Ma} = 0.5120 \pm 0.0001$), consistent with those of I-type plutonic rocks. The leucogranite has somewhat more positive εNd values, but equivalent $^{143}Nd/^{144}Nd_{300\ Ma}$ values, –5.6 to –4.6 and 0.5119–0.5120, respectively. The host metasedimentary sequence has very variable Nd isotope ratios. Calc-silicate and pelitic hornfelses of the Tamames Formation have crustal signatures, with εNd between –9.1 and –8.9 and $^{143}Nd/^{144}Nd_{300\ Ma}$ close to 0.5118. The underlying Upper Series have even more negative $\varepsilon Nd_{300\ Ma}$ values (–9.9 to –9.5) and $^{143}Nd/^{144}Nd_{300\ Ma}$ of 0.5118–0.5119. However, calculated $\varepsilon Nd_{300\ Ma}$ and $^{143}Nd/^{144}Nd_{300\ Ma}$ of the lowermost Lower Series are very different, –5.1 to –5.0 and 0.5120 (Ugidos *et al*. 1997b). The Nd isotopic values of the Los Santos scheelite are rather constant ($\varepsilon Nd_{300\ Ma}$, –9.4 to –8.5; $^{143}Nd/^{144}Nd_{300\ Ma}$, 0.5118). The prograde skarn and one sample of the endoskarn (plagioclase skarn) have similar εNd values (–9.7 to –8.5), whereas the other sample of endoskarn (LS–63) has more positive εNd values (–7), very likely indicating a predominant derivation of its Nd from the replaced granitic protolith.

As a whole, the granodiorite–monzogranite of the Spanish Central System has $^{87}Sr/^{86}Sr_i$ signatures between 0.7071 and 0.7192 and εNd_i close to –7.9 to –5.5 (Villaseca *et al*. 1998). The most evolved and peraluminous leucogranite (>70% SiO_2), which postdated the main plutonism and is related to the collapse of the orogen, has more ^{87}Sr-enriched values, in the range 0.7109–0.7254 (Ibarrola *et al*. 1988, Pérez Soba 1991, Villaseca *et al*. 1998). They have high REE contents (27–224 ppm; average 120 ppm) and markedly negative Eu anomalies (Eu/Eu* in the range 0.02–0.54, average 0.2).

The $^{87}Sr/^{86}Sr$ ratio of the scheelite at Los Santos at 300 Ma is rather constant, 0.7117–0.7119, and very similar to that of the associated endoskarn and exoskarn (0.7119–0.7129; Table 1). Most of these values are within the broad range defined by the replaced marble (0.7096) and the interbedded calc–

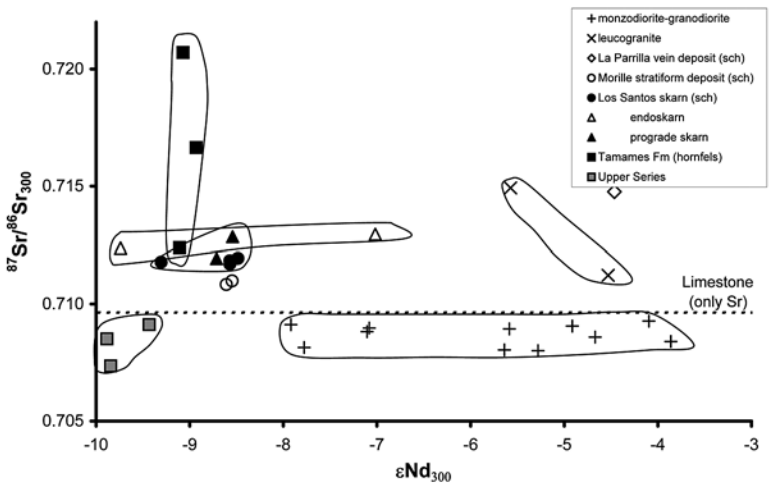

FIG. 7. Calculated εNd and $^{87}Sr/^{86}Sr$ values at 300 Ma of samples of skarn, the scheelite concentrate and the host rocks of Los Santos deposit. Regional data are from Pinarelli & Rottura (1995), Ugidos *et al*. (1997a) and Villaseca *et al*. (1998). SCS: Spanish Central System. CEG: Complejo Esquisto Grauváquico. Samples of the Lower Series are not shown owing to their low $^{87}Sr/^{86}Sr$ values.

silicate and pelitic hornfels (0.7124–0.7207) that form the bulk of the host rocks to the ore. In comparison with the underlying rocks, they are more radiogenic than the Upper Series ($^{87}Sr/^{86}Sr_{300\ Ma}$ in the range 0.7074–07091) and the Lower Series (<0.7000). The granitic rocks are also depleted in ^{87}Sr compared to the skarn ($^{87}Sr/^{86}Sr_{300\ Ma}$: 0.7087 ± 0.0003). The Sr isotopic ratio of the leucogranite, 0.7112–0.7149, matches that of the skarn, 0.7112–0.7129. Both the intense hydrothermal alteration, which probably disturbed the original isotopic ratios, and the high Rb/Sr values of the leucogranite (7–20; Table 1) suggest that these figures should be used with caution. However, and as quoted above, the regional data for the leucogranites show that these rocks usually have $^{87}Sr/^{86}Sr$ values even higher than those reported here.

In general, all the metasomatic rocks have low εNd and high $^{87}Sr/^{86}Sr_i$ ratios, indicating a dominant crustal derivation, either at the expense of the plutonic rocks or the hosting metasedimentary units, and excluding deep juvenile sources for fluids and metals. The calculated εNd – $^{87}Sr/^{86}Sr$ diagram at 300 Ma confirms that no unique fluid and metal reservoir can explain the observed features, and that the fluids involved in the formation of the skarn were derived from at least two sources with contrasting Nd and Sr isotope values.

The first source is characterized by low εNd values (<–9) and is likely represented by the late Vendian – Cambrian metasedimentary rocks of the area. Geochemically, it is not possible to distinguish the ultimate metasedimentary, low-εNd source of the fluids. Strontium could be derived from both the host hornfels and the replaced limestone or the Upper Series. However, and at a regional scale, it is more likely that interbedded carbonatic and pelitic rocks hosting the ore and showing widespread evidence of hydrothermal replacement have contributed some Sr to the final signature of the skarn. There is evidence that skarns, despite being formed at a very high fluid:rock ratio (>>1000), have most of their Sr inherited from their protolith (Bussell *et al*. 1990, Lieben *et al*. 2000). This is due to the high Sr contents of the carbonate rocks. Thus, migrating fluids would easily equilibrate their Sr isotope composition with the host rocks, partially masking the signature of the hydrothermal Sr. Some contribution of Sr from the Upper Series cannot be discounted, whereas *a priori*, the low $^{87}Sr/^{86}Sr$ and the high εNd values of the Lower Series exclude them as a likely source of the fluid. However, the skarn and the associated scheelite have high εNd values that are indicative of equilibration with another fluid characterized by εNd values higher than ~–8. The most likely candidates are the granitic rocks that crop out extensively nearby, either the granodiorite–monzogranite or the leucogranite. The granodiorite–monzogranite volumetrically dominates in the area and likely below the ore deposit, but shows no evidence of fluid exsolution nor major hydrothermal circulation. Fluids could thus equilibrate at low fluid:rock ratio during their circulation through this rock. However the leucogranite, despite being apparently volumetrically minor, is also a suitable candidate. Despite having major hydrothermal alteration that could mask the original isotopic signatures, regional comparison suggests that it could be the source of ^{87}Sr-enriched but Nd-depleted fluids.

Thus, the radiogenic isotope data are compatible with the derivation of Sr and Nd from the host metasedimentary rocks and the late Variscan granites. A broad numerical guess using the average Nd isotopic ratios and contents suggests that about 75% of the fluid was derived from the granite.

The low and constant Sm/Nd value of the skarn and related minerals at Los Santos causes all the isotope data to be aligned on a subhorizontal reference line on the $^{147}Sm/^{144}Nd$ *versus* $^{143}Nd/^{144}Nd$ diagram, thus leading to geologically meaningless ages. Similar behavior has been observed by Eichorn *et al*. (1997) in the Ferbertal deposit. The complex inheritance of Rb and Sr implies that the Rb–Sr isotope data also are scattered in the $^{87}Rb/^{86}Sr$ – $^{87}Sr/^{86}Sr$ diagram.

The stratabound scheelite mineralization at Morille has $\varepsilon Nd_{300\ Ma}$ (–8.6 and –8.7) and $^{87}Sr/^{86}Sr_{300\ Ma}$ (0.7108–0.7110) values that are very similar to those of Los Santos, indicating that they probably have a similar source and are of equivalent age. The slightly more juvenile signature of the Morille scheelite is interpreted to be due to the influence of the host rock, since the Upper Series has a somewhat more juvenile inheritance than the Tamames Formation. A pre-Variscan sedimentary-exhalative derivation, with no input from the Variscan granitic rocks, would imply signatures close to those of the host Upper Series at about 600–550 Ma. Calculated values for $^{87}Sr/^{86}Sr$ and εNd are near 0.7100 and –6, respectively, which depart from the calculated ones. Furthermore, hydrothermal remobilization and concentration of the syngenetic scheelite in the skarn would lead to low $^{87}Sr/^{86}Sr$ and εNd values. Thus, an ultimate pre-Variscan origin, with derivation of the Los Santos scheelite from a precursor Proterozoic mineralization represented by the Morille orebodies, is not acceptable, as the Sr and Nd data of both deposits are consistent with equilibration with fluids derived from the host metasedimentary and granitic rocks during Variscan times. In both cases, depleted mantle Nd model ages of scheelite calculated with the two-stage model of Borg *et al*. (1990) range between 1.65 and 1.6 Ga. These ages are equivalent to those calculated for the sediments of the Central Iberian Zone (e.g., Nägler 1990) and indicate that most of the Nd derives from long-lived crustal rocks.

The sample from La Parrilla has the highest $^{87}Sr/^{86}Sr$ and $\varepsilon Nd_{300\ Ma}$ values (0.71493 and –4.5, respectively), which are similar to those of the analyzed leucogranite (Fig. 7). The La Parrilla deposit overlies an unexposed leucogranite (Gumiel & Pineda 1981), and the veins are hosted by rocks equivalent to those of the Lower Series

(Ugidos *et al.* 1997a). The low εNd of the scheelite is consistent with derivation from the leucogranite and the Lower Series, with no input from metasedimentary units with stronger crustal affinities, such as the Upper Series or the Tamames Formation. Thus, the isotopic data are consistent with the regional geology and the genetic relationship of ^{87}Sr-enriched leucogranite and tungsten mineralization, supporting the existence of a hidden intrusion at depth beneath the La Parrilla deposit.

Discussion

The origin of metals and hydrothermal fluids

The ultimate origin of the hydrothermal fluids and tungsten at Los Santos is difficult to trace. The stable and radiogenic isotopes are consistent with the mixing of fluids equilibrated with the host rocks and an exotic fluid, likely equilibrated with the monzogranite–granodiorite or the leucogranite. As quoted above, the Sr isotope data of the leucogranite are probably disturbed during hydrothermal alteration, and do not allow discrimination between either magmatic sources.

The isotopic data alone are not conclusive, but the geological relationships strongly suggest that the mineralizing fluids equilibrated with the leucogranite. Key criteria include the enrichment of both fluorine and tungsten in the skarn, two elements typical of fluids equilibrated with evolved granites, the presence of a hydrothermally altered leucogranite, and the lack of scheelite mineralization away from this specific area. The leucogranite shows a direct spatial relationship with the mineralization, and the intrusive contacts of limestone with monzogranite–granodiorite away from the leucogranite are invariably barren. In fact, there is a systematic relationship of tungsten mineralization with late orogenic peraluminous leucogranite both in the Variscan Belt of Iberia (Kelly & Rye 1979, Derré *et al.* 1982, Mangas & Arribas 1988, Tornos & Gumiel 1992, Tornos *et al.* 2000) and elsewhere (Keith *et al.* 1989, Darbyshire & Shepherd 1985, Willis-Richards & Jackson 1989, Blevin & Chappell 1995, Heinrich 1995, Wayne *et al.* 1996, Smith *et al.* 1996). However, leucogranite is volumetrically minor in the area. It is difficult to envisage that the intrusions cropping out could have formed the skarn and exerted a strong influence on the Sr and Nd composition of the skarn. Thus, the existence of a deep unexposed pluton of leucogranite is proposed to be critical in the formation of the deposit. However, the isotopic and REE data are consistent with major chemical interchange with granodiorite–monzogranite and metasedimentary units, strongly suggesting that hydrothermal fluids interacted with regionally developed rocks prior to the mineralization. However, fluids would only precipitate scheelite, fluorite and REE when reacting with the carbonatic rocks, which increased the pH and the $a\mathrm{Ca}^{2+}/(a\mathrm{H}^{+})^{2}$. The evidence of significant fluorine metasomatism in the area presented by Timón *et al.* (2007) suggests that magmatic fluid percolated through the sequence, and metasomatism, more than simple distillation, was the main mechanism controlling the mineral assemblages near the skarn. It is difficult to envisage that such a large hydrothermal system was dominated by contact-metamorphic waters, and that these external fluids could leach tungsten from the regional rocks without producing major hydrothermal alteration at a regional scale.

In granitic systems, the absence of primary muscovite is interpreted to be a critical factor in the formation of magmatic tungsten mineralization. The crystallization of a granitic magma at relatively shallow depths in the absence of muscovite makes tungsten behave as an incompatible element, favoring partitioning into the hydrothermal phase, along with fluorine and other incompatible elements (Eugster 1985). Fluorine should dramatically lower the solidus temperature, allowing the shallow intrusion of the leucogranite despite relatively high H_2O contents (Dingwell 1988, Manning & Pichavant 1988). Furthermore, the composition of the hydrothermal fluid is consistent with the early exsolution of a magmatic fluid at relatively greater depths, below the H_2O–CO_2 immiscibility curve (see Bowers & Helgeson 1983).

However, there is little regional evidence of the circulation of magmatic fluids within the Spanish Central System. The dominant regional granodiorite–monzogranite is barren, and most of the mineralization is related to the shallow late orogenic leucogranite that was emplaced under H_2O-undersaturated conditions. Fluid-inclusion and stable isotope studies have shown that fluids circulating within these systems were of metamorphic (Reguilón *et al.* 2001, Villar *et al.* 2001) or surficial (Tornos *et al.* 2000) sources. Only minor evidence of circulation of magmatic fluids has been recorded (Vindel *et al.* 1995).

Environment of formation

During the formation of the Los Santos skarn, the fluid pressure was rather high (*ca.* 0.2 GPa; Timón *et al.* 2007), probably close to the lower limit for the formation of large hydrothermal systems. Several lines of evidence support a mesozonal environment of formation. They include: a) development of a stratabound skarn along major lithologic contacts and not as discordant bodies, b) absence of a major cross-cutting retrograde alteration that here seems to broadly, follow the same pathways as the prograde alteration, c) absence of contemporaneous quartz – scheelite – ferberite veins, d) isotopic composition of the fluids that suggests a deep source for fluids in both the early and late skarn, e) presence of two generations of scheelite in both the early and the retrograde skarn, a feature consistent with calculations on the solubility of this mineral at high pressures (*ca.* 2 kbar; Newberry & Swanson 1986), and

f) the contact-metamorphic assemblage (Rottura *et al.* 1989). The upper limit in fluid pressure is constrained by the absence of magmatic muscovite in the granitic rocks, near 3 kbar fluid pressure.

The sulfide and silicate assemblage of the skarn, with hedenbergitic pyroxene more abundant than granditic garnet, biotite and clinoamphibole dominant over epidote in the retrograde skarn, the low Mo content of the scheelite, the predominance of pyrrhotite and arsenopyrite over pyrite, and the relationship with ilmenite-bearing granite are all consistent with a reduced environment of formation. However, the REE data suggest that at least some of the Eu was transported as Eu^{3+} and, thus, the system was at least not highly reduced. Little is known about the relationships between the Eu^{3+}/Eu^{2+} ratio and the redox state of fluids at high temperatures.

The low sulfide content of the skarn is probably due to the low $f(S_2)$ and the high temperature of formation, both of which would inhibit the formation of significant amounts of sulfides. Furthermore, Candela (1997) has shown that in these reduced systems, Cu behaves as a compatible element, and residual fluids are enriched in W–Mo. The Sn-poor character of the skarn can be attributed to two factors: a) the relationship with intermediate to acid granites, which does not in every case show a concurrent enrichment in W and Sn (Einaudi *et al.* 1981, Meinert 1995), and b) the distal character of the skarn relative to an unexposed pluton. The geochemistry of the mineralization and the relationship with reduced peraluminous leucogranite show that the second alternative is more likely. A similar relationship of proximal W–Sn skarns and distal W-rich ones has been observed in the easternmost Spanish Central System (Casquet & Tornos 1984, 1991).

A factor of key importance in the formation of Los Santos skarn is the absence of isotopic evidence for circulation of surficial waters. Involvement of almost exclusively deep waters may be considered somewhat unusual, and only a few examples are recorded [*e.g.*, Mactung: Bowman (1998), Elkhorn: Bowman *et al.* (1985a), Cantung: Bowman *et al.* (1985b), Red Dome: Ewers & Sun (1989)]. The typical evolution of skarn includes a prograde stage dominated by the circulation of hot deep fluids and a later, retrograde stage associated with the inflow of cooler surficial waters that invade the hydrothermal system after the crystallization of the pluton, as has been described in the easternmost Spanish Central System (Tornos *et al.* 2000) and elsewhere (Einaudi *et al.* 1981, Kwak 1987, Meinert 1993, Bowman 1998, Meinert *et al.* 2005). Therefore, the Los Santos skarn represents a regionally unusual system exclusively related to the circulation of large amounts of deep fluids with a homogeneous isotopic signature.

The location of the Los Santos skarn in this specific context is interpreted as due to the focusing of significant amounts of deep fluids along a major tectonic discontinuity located at the contact between the granodiorite–monzogranite and the metasedimentary rocks. There is no regional evidence of major deformation (Yenes *et al.* 1999). However, the contact is parallel to the main strike-slip Variscan structures of the area. The existence of an extensional pull-apart zone in a left-lateral strike-slip structure is consistent with the inferred presence of a deep intrusive body, the existence of abundant subvertical NE-trending tensional faults controlling the location of quartz and aplitic dikes, and the morphology of the skarn zone. This hypothetical extensional structure triggered the emplacement of the unexposed granitic pluton and the related dikes, and channeled major flow of fluid.

The scarcity of other types of mineralization in the adjacent area is probably related to differential uplift and subsequent erosion during Alpine times. This orogeny produced block and fault tectonics with a "pop-up" morphology (Capote *et al.* 1990) that seems to be responsible for the different levels of erosion. This area is interpreted as an uplifted block compared with other nearby areas, where vein-type mineralization is much more abundant (*e.g.*, Mangas & Arribas 1987, Tornos *et al.* 2000). Thus only deep-seated deposits, such as skarns, can be found in these environments, whereas in shallower ones, hydrothermal veins are more widespread.

The radiogenic isotope data show that the stratabound mineralization at Morille has a different chemical signature than the host rocks but similar to that of the Los Santos skarn. This finding strongly suggests that mineralization in both cases is associated with leucogranite; we contend that the Los Santos deposit was not derived by the hydrothermal remobilization of the Morille mineralized zone. The deposits at Morille are interpreted as distal equivalents of the Los Santos skarn and formed in relationship to minor leucogranitic domes that crop out nearby. The fact that these intrusive bodies have related W veins suggests that these systems formed in much shallower conditions than those of the Los Santos skarn, where the formation of mineralized veins was inhibited by higher lithostatic pressures.

Conclusions

1) The Los Santos deposit is a classical mesozonal, Sn-poor and F-rich reduced tungsten-rich calcic skarn distal to the source granite. It shares many of the features of equivalent skarns elsewhere.

2) Combined radiogenic and stable isotope signatures and REE contents of the scheelite and the host rocks provide significant information on the origin and evolution of the ore-forming fluids in skarns. The model that best explains both geological and geochemical features includes the exsolution of F- and W-rich fluids from an underlying and sub-outcropping leucogranite intrusive body. These fluids extensively interacted with the pelitic and carbonate rocks of the Tamames Formation. Tungsten only precipitated by replacement

of the marble, where conditions of high pH and $a\mathrm{Ca}^{2+}/(a\mathrm{H}^{+})^{2}$ were attained. If that model holds true, then it would seem that tungsten-bearing fluids can travel large distances in the crust, even extensively interacting with the rocks, without causing significant mineralization.

3) The mesozonal formation of the skarn inhibited the circulation of low-temperature meteoric fluids and the formation of a retrograde skarn, with most of the scheelite concentrated in the prograde hedenbergite- and granditic-garnet-rich skarn.

4) The isotopic signatures of the scheelite from the skarn and the Morille stratabound mineralization are similar, but different from those of the host rocks, indicating that tungsten was likely derived from the plutonic rocks, and both styles of mineralization formed by similar processes. Thus, there is no geochemical evidence of the existence of a pre-Variscan exhalative tungsten mineralization.

Acknowledgements

The samples from the Morille mine were provided by Antonio Areas. This study was in part funded by the Spanish PB88–124 project and the Spanish–British Joint Action number 1995–033. We acknowledge suggestions and comments about the manuscript of P. Rodríguez, D.R. Lentz and N. Badham, and the reviews of A.K. Somarin, D.R. Lentz and R.F. Martin.

References

Anglin, C.D., Jonasson, I.R. & Franklin, J.M. (1996): Sm–Nd dating of scheelite and tourmaline: implications for the genesis of Archean gold deposits, Val d'Or, Canada. *Econ. Geol.* **91**, 1372-1382.

Arribas, A. (1979a): Los yacimientos de tungsteno de la zona de Morille (Provincia de Salamanca). *Chronique Recherche Minière* **459**, 27-34.

Arribas, A. (1979b): The Barruecopardo tungsten deposit. *Chronique Recherche Minière* **459**, 42-49.

Arribas, A. (1983): Geología y metalogenia del yacimiento Virgen de la Encina, Ponferrada, Leon. *Tecniterrae*, dec. 1983, 36-75.

Bell, K., Anglin, C.D. & Franklin, J.M. (1989): Sm–Nd and Rb–Sr isotope systematics of scheelites: possible implications for the age and genesis of vein-hosted gold deposits. *Geology* **17**, 500-504.

Blattner, P. & Lassey, K.R. (1989): Stable isotope exchange fronts, Damköhler numbers, and fluid to rock ratios. *Chem. Geol.* **78**, 381-392.

Blevin, P.L. & Chappell, B.W. (1995): Chemistry, origin, and evolution of mineralized granites in the Lachlan Fold belt, Australia: the metallogeny of I- and S-type granites. *Econ. Geol.* **90**, 1604-1619.

Borg, S.G., De Paolo, D.J. & Smith, B.M. (1990): Isotopic structure and tectonics of the Central Transantarctic Mountains. *J. Geophys. Res.* **95**, 6647-6667.

Borthwick, J. & Harmon, R. (1982): A note regarding ClF_3 as an alternative to BrF_5 for oxygen isotope analysis. *Geochim. Cosmochim. Acta* **46**, 1665-1668.

Bowers, T.S. & Helgeson, H.C. (1983): Calculation of the thermodynamic and geochemical consequences of nonideal mixing in the system H_2O–CO_2–NaCl on phase relations in geologic systems: equation of state for H_2O–CO_2–NaCl at high P and T. *Geochim. Cosmochim. Acta* **47**, 1247-1275.

Bowman, J.R. (1998): Stable-isotope systematics of skarns. *In* Mineralized Intrusion-Related Skarn Systems (D. Lentz, ed.). *Mineral. Assoc. Can., Short Course* **26**, 99-145.

Bowman, J.R., Covert, J.J., Clark, A.H. & Mathieson, G.A. (1985b): The Can Tung E zone scheelite skarn orebody, Tungsten, NW Territories: carbon, oxygen and hydrogen isotopic studies. *Econ. Geol.* **80**, 1872-1895.

Bowman, J.R., O'Neil, J.R. & Essene, E.J. (1985a): Contact skarn formation at Elkhorn, Montana. II. Origin and evolution of C–O–H skarn fluids. *Am. J. Sci.* **285**, 621-660.

Bussell, M.W., Alpers, C.N., Petersen, U., Shepherd, T.J., Bermudez, C. & Baxter, A.N. (1990): The Ag–Mn–Pb–Zn vein, replacement, and skarn deposits of Uchucchacua, Perú: studies of structure, mineralogy, metal zoning, Sr isotopes and fluid inclusions. *Econ. Geol.* **85**, 1348-1383.

Candela, P.A. (1997): A review of shallow, ore-related granites: textures, volatiles and ore metals. *J. Petrol.* **38**, 1619-1633.

Capote, R., Vicente, G. & González Casado, J.M. (1990): Evolución de las deformaciones alpinas en el Sistema Central Español. *Geogaceta* **7**, 20-22.

Casillas, R., Brandle, J.L., Huertas, M.J., Peinado, M., Pérez Soba, C. & Villaseca, C. (1991): Contenidos y variación de las tierras raras en los granitoides tardihercínicos de la Sierra de Guadarrama (SCE). *Boletín Sociedad Española Mineralogía* **14**, 251-272.

Casquet, C. & Tornos, F. (1984): El skarn de W–Sn del Carro del Diablo (Sistema Central Español). *Boletín Geológico Minero* **95**(1), 58-79.

Casquet, C. & Tornos, F. (1991): Influence of depth and igneous geochemistry on ore development in skarns: the Hercynian Belt of the Iberian Peninsula. *In* Skarns, their Petrology and Metallogeny (S.S. Augusthitis, ed.). Theophrastus Press, Athens, Greece (555-591).

Cheilletz, A. (1985): Les minéralisations stratiformes à scheelite–biotite du Djebel Aouaman (Maroc central). Exemple de skarn d'infiltration développé par remplacement de séries sédimentaires gréso-pélitiques. *Bull. Minéral.* **108**, 367-376.

CLAYTON, R.N. & MAYEDA, T.K. (1963): The use of bromine pentafluoride in the extraction of oxygen from oxides and silicates for isotopic analysis. *Geochim. Cosmochim. Acta* **27**, 43-52.

CRESPO, J.L., RODRÍGUEZ, P., MORO, M.C., CABRERA, R., CONDE, C., FERNÁNDEZ, A. & RODRÍGUEZ, I. (2000): El yacimiento de scheelita de Los Santos (Salamanca). *Geotemas* **1**(4), 25-28.

CULLERS, R.L. & GRAF, J.L. (1984): Rare earth elements in igneous rocks of the continental crust: intermediate to silicic rocks – ore petrogenesis. *In* Rare Element Geochemistry (P. Henderson, ed.). Elsevier, Amsterdam, The Netherlands (275-316).

DARBYSHIRE, D.P.F., PITFIELD, P.E.J. & CAMPBELL, S.D.G. (1996): Late Archean and Early Proterozoic gold–tungsten mineralization in the Zimbabwe Archean craton: Rb–Sr and Sm–Nd constraints. *Geology* **24**, 19-22.

DARBYSHIRE, D.P.F. & SHEPHERD, T.J. (1985): Chronology of granite magmatism and associated mineralization, SW England. *J. Geol. Soc. London* **142**, 1159-1177.

DELGADO, J.J., VENEMANN, T. & O'NEIL, J.R. (1994): The origin of metasomatic fluids in skarns from La Maladeta (Central Pyrenees, Spain): C, O, H, S and Sr isotopic compositions. *Mineral. Mag.* **58a**, 221-222.

DERRÉ, C., LÉCOLLE, M. & ROGER, G. (1982): Les quartzites à silicates calciques et scheelite: préconcentrations familières ou pièges pour un tungstène étranger lié à l'hydrothermalisme périgranitique? Exemple du nord-est Trasmontain (Portugal). *Mineral. Deposita* **17**, 363-385.

DÍEZ BALDA, M.D. (1980): La sucesión estratigráfica del Complejo Esquisto Grauvaquico al Sur de Salamanca. *Estudios Geologicos* **36**, 131-138.

DÍEZ BALDA, M.D., MARTÍNEZ CATALÁN, J.R., AYARZA, P. & ARRIBAS, P. (1995): Syn-collisional extensional collapse parallel to the orogenic trend in a domain of steep tectonics: the Salamanca detachment zone (Central Iberian Zone, Spain). *J. Struct. Geol.* **17**, 163-182.

DINGWELL, D.B. (1988): The structures and properties of fluorine-rich magmas: a review of experimental studies. *In* Recent Advances in the Geology of Granite-Related Mineral Deposits (R.P. Taylor & D.F. Strong, eds.). *Can. Inst. Mining Metall., Spec. Vol.* **39**, 1-12.

EICHORN, R., HOLL, R., JAGOUTZ, E. & SCHÄRER, U. (1997): Dating scheelite stages: a strontium, neodymium, lead approach from the Felbertal tungsten deposit, Central Alps, Austria. *Geochim. Cosmochim. Acta* **61**, 5005-5022.

EINAUDI, M.T., MEINERT, L.D. & NEWBERRY, R.J. (1981): Skarn deposits. *Econ. Geol., 75th Anniv. Vol.*, 317-391.

EUGSTER, H.P. (1985): Granites and hydrothermal ore deposits: a geochemical framework. *Mineral. Mag.* **49**, 7-23.

EWERS, G.R. & SUN, S.S. (1989): Genesis of the Red Dome gold skarn deposit, northeast Queensland. *In* The Geology of Gold Deposits: the Perspective in 1988. *Econ. Geol., Monogr.* **6**, 110-115.

FONTEILLES, M., SOLER, P., DEMANGE, M., DERRÉ, C., KRIER-SCHELLEN, A.D., VERKAEREN, J., GUY, B. & ZAHM, A. (1989): The scheelite skarn deposit of Salau (Ariège, French Pyrenees). *Econ. Geol.* **84**, 1172-1209.

FREI, R., NÄGLER, T.F., SCHÖNBERG, R. & KRAMERS, J.D. (1998): Re–Os, Sm–Nd, U–Pb and stepwise lead leaching isotope systematics in shear zone hosted gold mineralization: genetic tracing and age constraints of crustal hydrothermal activity. *Geochim. Cosmochim. Acta* **62**, 1925-1936.

FRIEDMAN, I. & O'NEIL, J.R. (1977): Compilation of stable isotope fractionation factors of geochemical interest. *In* Data of Geochemistry (M. Fleischer, ed.). *U.S. Geol. Surv., Prof. Pap.* **440–KK**.

GASPAR, M.L. & INVERNO, C.M.C. (2000): Mineralogy and metasomatic evolution of distal strata-bound scheelite skarns in the Riba de Alva mine, NE Portugal. *Econ. Geol.* **95**, 1259-1275.

GHADERI, M., PALIN, J.M., CAMPBELL, I.H. & SYLVESTER, P.J. (1999): Rare earth element systematics in scheelite from hydrothermal gold deposits in the Kalgoorlie–Norseman region, Western Australia. *Econ. Geol.* **94**, 423-437.

GIERÉ, R. (1986): Zirconolite, allanite and hoegbomite in a marble skarn from the Bergell contact aureole: implications for mobility of Ti, Zr and REE. *Contrib. Mineral. Petrol.* **93**, 459-470.

GIULIANI, G., CHEILLETZ, A. & MECHICHE, M. (1987): Behaviour of REE during thermal metamorphism and hydrothermal infiltration associated with skarn and vein-type tungsten ore bodies in central Morocco. *Chem. Geol.* **64**, 279-294.

GUMIEL, P. & PINEDA, A. (1981): Estudio del yacimiento de scheelita de La Parrilla (Cáceres–Badajoz). *Tecniterrae* **S–259**.

GUY, B. (1979): *Pétrologie et géochimie isotopique (S,C,O) des skarns à scheelite de Costabonne*. Thèse de doctorat, ENSM, Paris, France.

HANSON, G. (1980): REE in petrogenetic studies of igneous systems. *Annu. Rev. Earth Planet. Sci.* **8**, 371-406.

HEINRICH, C.A. (1995): Geochemical evolution and hydrothermal mineral deposition in Sn(–W–base metal) and other granite-related ore systems: some conclusions from Australian examples. *In* Magmas, Fluids and Ore Deposits (J.F.H. Thompson, ed.). *Mineral. Assoc. Can., Short Course* **23**, 203-220.

IBARROLA, E., VILLASECA, C., VIALETTE, Y., FÚSTER, J.M., NAVIDAD, M., PEINADO, M. & CASQUET, C. (1988): Dating of Hercynian granites in the Sierra de Guadarrama

(Spanish Central System). *In* Geología de los Granitoides y Rocas Asociadas del Macizo-Hespérico. Rueda, Madrid, Spain (377-383).

IGME (1985): Inventario nacional de los recursos de volframio. IGME, Madrid, Spain.

KEITH, J.D., VAN MIDDELAAR, W., CLARK, A.H. & HODGSON, C.J. (1989): Granitoid textures, compositions and volatile fugacities associated with the formation of tungsten-dominated skarn deposits. *In* Ore Deposition Associated with Magmas (J.A. Whitney & A.J. Naldrett, eds.). *Rev. Econ. Geol.* **4**, 235-250.

KELLY, W.C. & RYE, R.O. (1979): Geologic, fluid inclusion and stable isotope studies of the tin–tungsten deposits of Panasqueira, Portugal. *Econ. Geol.* **74**, 1721-1822.

KEMPE, U., BELYATSKI, B.V., KRYMSKY, R.S., KREMENETSKY, A.A. & IVANOV, P.A. (2001): Sm–Nd and Sr isotope systematics of scheelite from the giant Au–(W) deposit Muruntau (Uzbekistan): implications for the age and sources of Au mineralization. *Mineral. Deposita* **36**, 379-392.

KENT, A.J.R., CAMPBELL, I.H. & MCCULLOCH, M.T. (1995): Sm–Nd systematics of hydrothermal scheelite from the Mount Charlotte mine, Kalgoorlie, Western Australia: an isotopic link between gold mineralization and komatiites. *Econ. Geol.* **90**, 2329-2335.

KWAK, T.A.P. (1987): *W–Sn Skarn Deposits and Related Metamorphic Skarns and Granitoids*. Elsevier, Amsterdam, The Netherlands.

LIEBEN, F., MORITZ, R. & FONTBOTÉ, L. (2000): Mineralogy, geochemistry and age constraints on the Zn–Pb skarn deposit of Maria Cristina, Quebrada Galena, northern Chile. *Econ. Geol.* **95**, 1185-1196.

MANGAS, J. & ARRIBAS, A. (1987): Fluid inclusion study in different types of tin deposits associated with the Hercynian granites of western Spain. *Chem. Geol.* **61**, 193-208.

MANGAS, J. & ARRIBAS, A. (1988): Hydrothermal fluid evolution of the Sn–W mineralization in the Parrilla ore deposit (Cáceres, Spain). *J. Geol. Soc. London* **145**, 147-155.

MANNING, D.A.C. & PICHAVANT, M. (1988): Volatiles and their bearing on the behaviour of metals in granitic systems. *In* Recent Advances in the Geology of Granite-Related Mineral Deposits (R.P. Taylor & D.F. Strong, eds.). *Can. Inst. Mining Metall., Spec. Vol.* **39**, 13-24.

MEINERT, L.D. (1993): Skarns and skarn deposits. *In* Ore Deposit Models II (P. Sheahan & M.E. Cherry, eds.). *Geosci. Can., Reprint Ser.* **6**, 117-134.

MEINERT, L.D. (1995): Compositional variations of igneous rocks associated with skarn deposits. Chemical evidence fro a genetic connection between petrogenesis and mineralization. *In* Magmas, Fluids and Ore Deposits (J.F.H. Thompson, ed.). *Mineral. Assoc. Can., Short Course* **23**, 401-418.

MEINERT, L.D., DIPPLE, G.M. & NICOLESCU, S. (2005): World skarn deposits. *In* Economic Geology – One Hundredth Anniversary Volume (J.W. Hedenquist, J.F.H. Thompson, R.J. Goldfarb & J.P. Richards, eds.). Society of Economic Geologists, Littleton, Colorado (299-336).

MUELLER, A.G., GROVES, D.I. & DELOR, C.P. (1991): The Savage Lode magnesian skarn in the Marvel Loch gold–silver mine, Southern Cross greenstone belt, Western Australia. II. Pressure–temperature estimates and constraints of fluid sources. *Can. J. Earth Sci.* **28**, 686-705.

NÄGLER, T. (1990): *Sm–Nd, Rb–Sr and Common Lead Isotope Geochemistry on Fine-Grained Sediments of the Iberian Massif*. Ph.D. thesis, Swiss Federal Institute Technology, Zurich, Switzerland.

NEWBERRY, R.J. & SWANSON, S.E. (1986): Scheelite skarn granitoids: an evaluation of the roles of magmatic source and process. *Ore Geol. Rev.* **1**, 57-81.

NIE, F.J. (1994): Rare earth element geochemistry of the molybdenum-bearing granitoids in the Jinduicheng–Haunglongpu district, Shaanxi Province, northwest China. *Mineral. Deposita* **29**, 488-498.

OBERTHUR, T., BLENKINSOP, T.G., HEIN, H.F., HOPPNER, M., HOHNDORF, A. & WEISER, T.W. (2000): Gold mineralization in the Mazowe area, Harare–Bindura–Shamva greenstone belt. Zimbabwe. II. Genetic relationships deduced from mineralogical, fluid inclusion and stable isotope studies, and the Sm–Nd isotopic composition of scheelites. *Mineral. Deposita* **35**, 138-156.

PAN, YUANMING & DONG, PING (1999): The Lower Changjiang (Yangzi/Yangtze River) metallogenic belt, east central China: intrusion- and wall rock-hosted Cu–Fe–Au, Mo, Zn, Pb, Ag deposits. *Ore Geol. Rev.* **15**, 177-242.

PAN, YUANMING & FLEET, M.F. (1992): Calc-silicate alteration in the Hemlo gold deposit, Ontario: mineral assemblages, P–T–X contraints and significance of formation. *Econ. Geol.* **87**, 1104-1121.

PELLITERO, E., SAAVEDRA, J., GARCÍA SÁNCHEZ, A. & GONZALO CORRAL, F. (1984): Caracterización de concentraciones estratiformes de Sn y W en la zona de S. Pedro de Rozados – Martinamor (Salamanca). *Cuaderno Laboratorio Xeoloxico Laxe* **9**, 177-189.

PÉREZ SOBA, C. (1991): *Petrología y Geoquímica del Macizo Granítico de La Pedriza*. Ph.D. thesis, Univ. Complutense Madrid, Madrid, Spain.

PINARELLI, L. & ROTTURA, A. (1995): Sr and Nd isotopic study and Rb–Sr geochronology of the Bejar granites, Iberian Massif, Spain. *Eur. J. Mineral.* **7**, 577-589.

PINTO, A.F. (1986): Trace element geochemistry of calcsilicate rocks from N and central Portugal. *Comunicaçoes Servicio Geologico Portugal* **71**, 187-196.

POITRASSON, F., PIN, C. & DUTHOU, J.-L. (1995): Hydrothermal remobilization of rare earth elements and its effect on Nd

isotopes in rhyolite and granite. *Earth Planet. Sci. Lett.* **130**, 1-11.

RECIO, C., FALLICK, A.E. & UGIDOS, J.M. (1992): A stable isotopic ($\delta^{18}O$, δD) study of the late Hercynian granites and their host-rocks in the Central Iberian Massif (Spain). *Trans. R. Soc. Edinb.: Earth Sci.* **83**, 247-257.

REGUILÓN, R., RODRÍGUEZ, I., MANGAS, J. & JIMENEZ, E. (2001): Caracterización de los fluidos mineralizadores de "Mina Saturno", Valderrodrigo (Salamanca). *Bol. Soc. Española Mineral.* **24-A**, 165-166.

RODA ROBLES, E., PESQUERA PEREZ, A., VELASCO ROLDAN, F. & FONTAN, F. (1999): The granitic pegmatites of the Fregeneda area (Salamanca, Spain): characteristics and petrogenesis. *Mineral. Mag.* **63**, 535-558.

ROSE, A.W., KERRICK, D.C. & DEINES, P. (1985): An oxygen and sulfur isotope study of skarn-type magnetite deposits of the Cornwall type, southeastern Pennsylvania. *Econ. Geol.* **80**, 418-443.

ROTTURA, A., BARGOSSI, G.M., CAIRONI, V., D'AMICO, C. & MACCARRONE, E. (1989): Petrology and geochemistry of late-Hercynian granites from the Western Central System of the Iberian Massif. *Eur. J. Mineral.* **1**, 667-683.

SERRANO PINTO, M., CASQUET, C., IBARROLA, E., CORRETGÉ, L.G. & PORTUGAL FERREIRA, M. (1988): Sintese geocronologica dos granitoides do Macizo Hespérico. *In* Geología de Los Granitoides y Rocas Asociadas del Macizo Hespérico. Rueda, Madrid, Spain (69-86).

SHEPPARD, S.M.F. (1986): Characterization and isotopic variations in natural waters. *In* Stable Isotopes in High Temperature Geological Processes (J.W. Valley, H.P. Taylor, Jr. & J.R. O'Neil, eds.). *Rev. Mineral.* **16**, 165-183.

SMITH, M., BANKS, D.A., YARDLEY, B.W. & BOYCE, A.J. (1996): Fluid inclusion and stable isotope constraints on the genesis of the Cligga Head Sn–W deposit, SW England. *Eur. J. Mineral.* **8**, 961-974.

SMITH, M.P., HENDERSON, P., JEFFRIES, T.E.R., LONG, J. & WILLIAMS, C.T. (2004): The rare earth elements and uranium in garnets from the Beinn and Dubhaich aureole, Skye, Scotland, UK: constraints on processes in a dynamic hydrothermal system. *J. Petrol.* **45**, 457-484.

SOLER, A., AYORA, C., CARDELLACH, E. & DELGADO, J. (1990): Gold bearing hedenbergite skarns from the SW contact of the Andorra granite (Central Pyrenees, Spain). *Mineral. Deposita* **25** (suppl.), S59-S68.

SOLER, P. (1980): Géologie du gisement de Salau. *Bur. Rech. Géol. Minières, Mém.* **99**, 205-229.

SVERJENSKY, D.A. (1984): Europium redox equilibria in aqueous solutions. *Earth Planet. Sci. Lett.* **67**, 70-78.

TIMÓN, S.M., MORO, M.C., CEMBRANOS, M.L., FERNÁNDEZ, A. & CRESPO, J.L. (2007): Contact metamorphism in the Los Santos W skarn (NW Spain). *Mineral. Petrol.* **90**, 109-140.

TORNOS, F., DELGADO, A., CASQUET, C. & GALINDO, C. (2000): 300 Million years of episodic hydrothermal activity: stable isotope evidence from hydrothermal rocks of the eastern Iberian Central System. *Mineral. Deposita* **35**, 551-569.

TORNOS, F. & GUMIEL, P. (1992): El wolframio y estaño: aspectos económicos y metalogénicos. *In* Recursos Minerales de España, Textos Universitarios CSIC **15**, 379-394.

UGIDOS, J.M., ARMENTEROS, I., BARBA, P., VALLADARES, M.I. & COLMENERO, J.R. (1997a): Geochemistry and petrology of recycled orogen-derived sediments: a case study from Upper Precambrian siliciclastic rocks of the Central Iberian Zone, Iberian Massif, Spain. *Precamb. Res.* **84**, 163-180.

UGIDOS, J.M. & RECIO, C. (1993): Origin of cordierite-bearing granites by assimilation in the Central Iberian Massif (CIM), Spain. *Chem. Geol.* **103**, 27-43.

UGIDOS, J.M., VALLADARES, M.I., RECIO, C., ROGERS, D., FALLICK, A.E. & STEPHENS, W.E. (1997b): Provenance of Upper Precambrian – Lower Cambrian shales in the Central Iberian Zone, Spain: evidence from a chemical and isotopic study. *Chem. Geol.* **136**, 55-70.

VALLADARES, M.I., UGIDOS, J.M., BARBA, P. & COLMENERO, J.R. (2002): Contrasting geochemical features of the Central Iberian Zone shales (Iberian Massif, Spain): implications for the evolution of Neoproterozoic – Lower Cambrian sediments and their sources in other peri-Gondwana areas. *Tectonophysics* **353**, 121-132.

VAN DER AUWERA, J. & ANDRÉ, L. (1991): Trace elements (REE) and isotopes (O, C, Sr) to characterize the metasomatic fluid sources: evidence from the skarn deposit (Fe, W, Cu) of Traversella (Ivrea, Italy). *Contrib. Mineral. Petrol.* **106**, 325-339.

VENNEMAN, T. & SMITH, H. (1990): The rate and temperature of reaction of ClF_3 with silicate minerals, and their relevance to oxygen isotope analysis. *Chem. Geol.* **86**, 83-88.

VILADEVALL, M., SAAVEDRA, J. & PELLITERO, E. (1980): Scheelita en el contacto granítico Monleón – Los Santos (Salamanca): Consideraciones genéticas. *Tecniterrae* **37**, 29-33.

VILLAR, P., MORO, M.C., FERNÁNDEZ, A., FADÓN, O., CRESPO, J.L. & CEMBRANOS, M.L. (2001): Caracterización y geotermometría isotópicas de las mineralizaciones de W–As-Au del distrito de Barruecopardo (O de Salamanca). *Bol. Soc. Española Mineral.* **24-A**, 167-168.

VILLASECA, C., BARBERO, L. & ROGERS, G. (1998): Crustal origin of Hercynian peraluminous granitic batholiths of central Spain: petrological, geochemical and isotopic (Sr, Nd) constraints. *Lithos* **43**, 55-79.

VINDEL, E., LOPEZ, J.A., BOIRON, M.-C., CATHELINEAU, M. & PRIETO, A.C. (1995): P–V–T–X–fO_2 evolution from

wolframite to sulphide depositional stages in intragranitic W-veins; an example from the Spanish Central System. *Eur. J. Mineral.* **7**, 675-688.

VOICU, G., BARDOUX, M., STEVENSON, R. & JÉBRAK, M. (2000): Nd and Sr study of hydrothermal scheelite and host rocks at Omai, Guiana Shield: implications for ore fluid source and flow path during the formation of orogenic gold deposits. *Mineral. Deposita* **35**, 302-314.

YENES, M., ÁLVAREZ, F. & GÚTIERREZ-ALONSO, G. (1999): Granite emplacement in orogenic compressional conditions: the Alberca–Béjar granitic area (Spanish Central System, Variscan Iberian Belt). *J. Struct. Geol.* **21**, 1419-1440.

WALTHER, J.V. & HELGESON, H.C. (1977): Calculation of the thermodynamic properties of aqueous silica and the solubility of quartz and its polymorphs at high pressure and temperatures. *Am. J. Sci.* **277**, 1315-1351.

WANG, SHIQI & WILLIAMS, P.J. (2001): Geochemistry and origin of Proterozoic skarns at the Mount Elliot Cu–Au(–Co–Ni) deposit, Cloncurry district, NW Queensland, Australia. *Mineral. Deposita* **36**, 109-124.

WAYNE, D.M., MILLER, M.F., SCRIVERENER, R.C. & BANKS, D.A. (1996): U–Pb and Rb–Sr isotopic systematics of fluids associated with mineralization of the Dartmoor granite, SW England. *Geochim. Cosmochim. Acta* **60**, 653-666.

WILLIS-RICHARD, S,J. & JACKSON, N.J. (1989): Evolution of the Cornubian ore field, southwest England. I. Batholith modeling and ore distribution. *Econ. Geol.* **84**, 1078-1100.

ZHENG, YONG-FEI (1993): Calculation of oxygen isotope fractionation in anhydrous silicate minerals. *Geochim. Cosmochim. Acta* **57**, 1079-1091.

ZÜRCHER, L., RUIZ, J. & BARTON, M.D. (2001): Paragenesis, elemental distribution and stable isotopes at the Peña Colorada iron skarn, Colima, Mexico. *Econ. Geol.* **96**, 535-557.

Received June 6, 2007, revised manuscript accepted January 1, 2008.